A model for $\pi\Delta$ electroproduction on the proton

J.C. Nacher and E. Oset

Departamento de Física Teórica and IFIC

Centro Mixto Universidad de Valencia-CSIC

46100 Burjassot (Valencia)

Spain.

Abstract

We have extended a model for the $\gamma N \to \pi\pi N$ reaction to virtual photons and selected the diagrams which have a Δ in the final state. With this model we have evaluated cross sections for the virtual photon cross section as a function of Q^2 for different energies. The agreement found with the $\gamma_v p \to \Delta^0\pi^+$ and $\gamma_v p \to \Delta^{++}\pi^-$ reactions is good. The sensitivity of the results to $N\Delta$ transition form factors is also studied. The present reaction, selecting a particular final state, is an extra test for models of the $\gamma_v N \to \pi\pi N$ amplitude. The experimental measurement of the different isospin channels for this reaction are encouraged as a means to unravel the dynamics of the two pions photoproduction processes.

1 Introduction

The $\gamma N \to \pi\pi N$ reaction in nuclei has captured some attention recently and has proved to be a source of information on several aspects of resonance formation and decay as well as a test for chiral perturbation theory at low energies. A model for the $\gamma p \to \pi^+\pi^- p$ reaction was developed in [1] containing 67 Feynman diagrams by means of which a good reproduction of the cross section was found up to about $E_\gamma \simeq 1$ GeV.

A more reduced set of diagrams, with 20 terms , was found sufficient to describe the reaction up to $E_\gamma \simeq 800$ MeV [2] where the Mainz experiments are done [3,4,5].

In the same work [2] the model was extended to the other charge channels of $(\gamma, 2\pi)$ and the agreement with the experiment is good except for the channel $\gamma p \to \pi^+\pi^0 n$ where the theoretical cross section underestimates the experiment in about 40 per cent.

Other models have also been recently proposed. The model of ref. [6] contains the dominant terms of [1] and includes some extra resonances in order to make predictions at high energies. A prescription to approximately unitarize the model, of relevance at high energies, is also proposed. Revision of this work is under consideration [7], so more about it should be known in the future.

The model of [8] has fewer diagrams than the one of [1,2] but introduces the $N^*(1520) \to N\rho$ decay mode. By fitting a few parameters to $(\gamma, \pi\pi)$ data the cross sections are reproduced, including the $\gamma p \to \pi^+\pi^0 n$ reaction where the model of [2] fails. The $(\gamma, \pi^0\pi^0)$ channel is somewhat underpredicted. The model of [8] fails to reproduce some invariant mass distributions where the model of [1] shows no problems. A different version of the model of [8] is given in [9], where the parameters of the model are changed in order to reproduce the mass distribution, without spoiling the cross sections. One of the problems in the fit of [9] is that the range parameter of the ρ coupling to baryons is very small, around 200 MeV, which would not be easily accomodated in other areas of the ρ phenomenology, like the isovector πN $s-wave$ scattering amplitude.

On the other hand the model of [2] has no free parameters. All input is obtained from known properties of resonances and their decay, with some unknown sign borrowed from quark models. With all its global success in the different isospin channels, the persistance of the discrepancy in the $\gamma p \to \pi^+\pi^0 n$ channel indicates that further work is needed. The constraints provided by the data in two pion electroproduction should be useful to further test present models and learn more about the dynamics of the two pion production.

The $(\gamma,2\pi)$ reaction has also been used to test chiral perturbation theory. The threshold region is investigated in [10,11] with some discrepancies in the results which are commented in [12,13]. The one loop corrections are shown to be relevant in the $\gamma p \to \pi^0\pi^0 p$ reaction close to threshold [11]. In addition the $N^*(1440)$ excitation is shown to be very important at threshold in [2].

Another interesting information obtained from the $\gamma p \to \pi^+\pi^- p$ reaction is

information about the $N^*(1520)$ decay into $\Delta\pi$. Indeed, the photoexcitation of the $N^*(1520)$ followed by the decay into $\Delta\pi$ is a mechanism which interferes with the dominant term, the $\gamma N\Delta\pi$ Kroll-Ruderman term, and offers information on the q dependence and the sign of the s and $d-wave$ amplitudes of $N^*(1520) \to \Delta N$ decay. This information is a good test of quark models [14] which is passed by the "relativised" constituent quark models [15,16,17]. In the $\gamma p \to \pi^0\pi^0 p$ reaction the $\gamma N \to N^*(1520) \to \Delta\pi$ is shown to be an important mechanism by itself (there is no Δ Kroll-Ruderman term here), and it is perfectly visible in the experimental invariant mass distribution [5].

The (γ,2π) reaction has also relevance in nuclear physics. Inclusive cross section for the (γ,$\pi^+\pi^-$) have been calculated in [18] and the inclusive (γ,$\pi^0\pi^0$) reaction is measured in [19]. Calculations for (γ,$\pi^+\pi^-$) and the (γ,$\pi^0\pi^0$) coherent two pion production in nuclei have been performed in [20] and the cross sections are found to be very different in two different charge channels, with patterns in the energy and angular distributions linked to isospin conservation. Similarly, exchange currents for the (γ,π^+) reaction are constructed from (γ,$\pi\pi$) when a pion is produced off-shell and absorbed by a second nucleon. These exchange currents give an important contribution to the (γ,π^+) cross section at large momentum transfer [21].

The discussions above have served to show the relevance of the (γ,2π) reaction and its implications in different processes. The extension of this kind of work to virtual photons should complement the knowledge obtained through the (γ,2π) and the related reactions. The coupling of the photons to the resonances depends on q^2 and the dependence can be different for different resonances. Hence, the interference of different mechanisms pointed above will depend on q^2 and with a sufficiently large range of q^2, one can pin down the mechanism of (γ,2π) with real or virtual photons with more precision than just with real photons, which would help settle the differences between present theoretical models.

However, there are already interesting two pion electroproduction experiments selecting Δ in the final state. The reactions are, $ep \to e'\pi^+\Delta^{++}$ and $ep \to e'\pi^+\Delta^0$ [22]. It is thus quite interesting to extend present models of $(\gamma, 2\pi)$ to the realm of virtual phtons and compare with existing data. In the present paper we do so, extending the model of ref.[2] to deal with the electroproduction process. This model is flexible enough and one can select the diagrams which contain $\Delta\pi$ in the final state in order to compare directly with the measured cross sections.

The extension of the model requires three new ingredients: the introduction of the zeroth component of the photon coupling to resonances (calculations where done in [2] in the Coulomb gauge, ϵ^0, where the zeroth component is not needed), the implementation of the q^2 dependence of the amplitudes, which will be discussed in forthcoming sessions, and the addition of the explicit terms linked to the $S_{1/2}$ helicity amplitudes which vanish for real photons.

Experiments on (γ_v,2π) are presently being done in the Thomas Jefferson Laboratory [23], both for $N\Delta$ and $N\pi\pi$ production.

The model presented here can serve to extract relevant information from coming data, which will improve appreciably the precission of present experiments.

There has been earlier work on the particular problem which we are discussing here. In [24] an approach for $\Delta\pi$ electroproduction close to threshold was done with special emphasis in determining the axial transition form factors. The approach uses the current algebra formalism and some of the input needed is obtained from the same electroproduction data. The delta is treated as an elementary particle but the cross sections are folded with a Breit Wigner distribution in order to take into account approximately the effects of the finite width of the Δ. The effects of the D_{13} resonance are also discussed and introduced in an approximate way. The novelties here with respect to this work would be the use of a different formalism, since we are relying on the Feynman diagrammatic approach. On the other hand all information needed here, some of which was not available at the time of ref.[24], is already known such that clear predictions can be made. There is another important difference with respect to [24] which is that the Δ is not considered as a final state but decays explicitly into πN in the Feynman diagrams considered. This means that the Δ is treated as a propagator and the sum over polarizations is done in the amplitudes not in the cross sections as in [24]. This allows one to keep track of angular correlations between the two pions which are lost if the Δ is considered as a final state. It also allows to take into account the delta width in a natural way since it just comes as the imaginary part of the inverse of the Δ propagator. It also allows one to keep track of interference of different pieces, in particular those between the Δ Kroll Ruderman term and the excitation of the $N^*(1520)$ resonance followed by $\Delta\pi$ decay, which is one of the important findings in the present reaction.

Our model bears more similarity to the work of [25] where also a diagrammatic approach is followed. They introduce the minimal set of terms which are gauge invariant as a block, including the important Δ Kroll Ruderman term. In our model we also include the four terms of [25] but we have in addition four more terms, in particular the excitation of the $N^*(1520)$ resonance followed by $\Delta\pi$ decay, which has a strong interference with the Δ Kroll Ruderman term. In [25] a formalism is used which respects Ward identities and leads to a gauge invariant amplitude in the presence of different electromagnetic form factors for the different terms of the model appearing for virtual photons. We have also followed this formalism in our approach.

For the construction of the currents for resonance excitation we follow closely the work of [26] and take the convention of [27] for the definition of the helicity amplitudes. Altogether the formalism in the present paper diverts somewhat from the one used for real photons in [1,2] where many simplifications could be done, but in the case of real photons we regain the results of [1,2], although the use of new conventions forces the change of some sign. In order to avoid confusion the Lagrangians used and new conventions are now written in detail in a section.

2 Model for $eN \to e'\Delta\pi$.

We will evaluate cross sections of virtual photons integrated over all the variables of the pions and the outgoing nucleon. In this case the formalism is identical to the one of inclusive $eN \to e'X$ scattering [28,29] or pion electroproduction after integrating over the pion variables [30,31]. The (e, e') cross section is given by

$$\begin{aligned} \frac{d\sigma}{d\Omega' dE'} &= \frac{\alpha^2}{q^4}\frac{k'}{k}\frac{-q^2}{1-\epsilon}\frac{1}{2\pi e^2}[(W^{xx}+W^{yy})+ \\ &\quad 2\epsilon(\frac{-q^2}{\vec{q}^2})W^{00}] \end{aligned} \tag{1}$$

where $\alpha = e^2/4\pi$ is the fine structure constant, e the electron charge, q^μ the momentum of the virtual photon and k, k' the momenta of the initial and the final electron and ϵ the polarization parameter of the photon, which is given by

$$\epsilon = [1 - \frac{2\vec{q}^2}{q^2} tg^2 \frac{\theta_e}{2}]^{-1} \tag{2}$$

with θ_e the angle of the scattered electron. All variables are given in the lab frame and the z direction is taken along the direction of the virtual photon, $\vec{q}$. Furthermore, the hadronic tensor is given here by

$$\begin{aligned} W^{\mu\nu} &= \int \frac{d^3p_2}{(2\pi)^3}\frac{M}{E_1}\frac{M}{E_2}\int \frac{d^3p_4}{(2\pi)^3}\frac{1}{2w_4}\int \frac{d^3p_5}{(2\pi)^3}\frac{1}{2w_5} \\ &\quad \overline{\sum}\sum T^\mu T^{\nu *}(2\pi)^4\delta(q+p_1-p_2-p_4-p_5) \end{aligned} \tag{3}$$

where p_1, p_2, p_4, p_5 are the momenta of the initial, final nucleon, and the two pions and T^μ is the matrix element of the $\gamma_v N_1 \to N_2\pi_4\pi_5$ process. Note that the phase space accounts for the decay of the Δ into $N\pi$ explicitly, hence the finite width of the Δ is automatically taken into account. The terms contributing to T^μ are given below.

The expression of eq.(1) can be conveniently rewritten as [30]

$$\frac{d\sigma}{d\Omega' dE'} = \Gamma(\sigma^T_{\gamma_v} + \epsilon\sigma^L_{\gamma_v}) = \Gamma\sigma_{\gamma_v} \tag{4}$$

where $\sigma^T_{\gamma_v}$, $\sigma^L_{\gamma_v}$ are the transverse,longitudinal cross sections of the virtual photons and Γ is given by

$$\Gamma = \frac{\alpha}{2\pi^2}\frac{1}{-q^2}\frac{k'}{k}\frac{1}{1-\epsilon}K_\gamma \tag{5}$$

$$K_\gamma = \frac{s-M^2}{2M} \quad ; s = (q^0+M)^2 - \vec{q}^2 \tag{6}$$

The corresponding cross sections $\sigma^T_{\gamma_v}$ and $\sigma^L_{\gamma_v}$ are easily induced from eqs. (1) and (4). The term with the combination $W^{xx} + W^{yy}$ in eq. (1) gives rise

to the transverse cross section while the term proportional to W^{00} gives rise to the longitudinal one.

In the limit of the real photons, when $q^2 \simeq 0$, K_γ is the lab momentum of the photon, and only the transverse cross section contributes, in which case $\sigma^T_{\gamma_v} = \sigma_\gamma$, the cross section of real photons.

For the model of the $\gamma_v N \to \Delta\pi$ reaction we take the same diagrammatic approach as in ref.[2] and select the diagrams which have a Δ in the final state. The diagrams which contribute to the process are depicted in fig.1. The contribution of each one of the diagrams is readily evaluated from the Lagrangians written in appendix A1. The Feynman rules for the diagrams are collected in appendix A2. The coefficients, coupling constants and the form factors are collected in appendix A3. Finally, the amplitudes for each one of the terms are written in appendix A4 for each charge state.

Out of the 20 terms in [2] for the general $(\gamma, 2\pi)$ reaction only 8 terms contain a Δ and a pion in the final state which are the terms collected in fig.1.

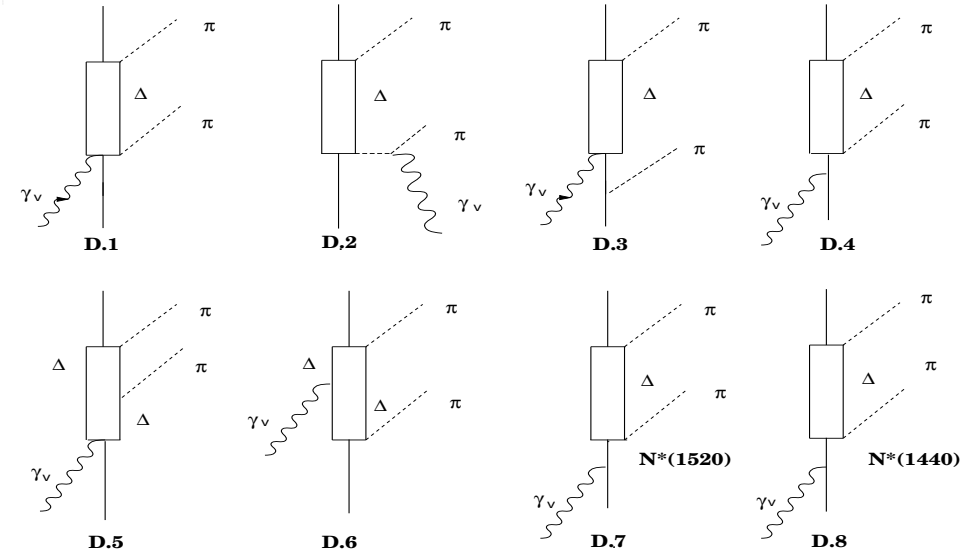

Fig.1

Figure 1: Feynman diagrams used in the model for $\gamma_v p \to \pi\Delta$

3 Electromagnetic transitions for Roper and N*(1520) resonances

We follow the paper from Devenish et al. [26] in our approach to these transitions. As we are working with virtual photons we need to care about these couplings and hence include terms which vanish for real photons. For the diagram D.8, which involves the Roper excitation as depicted in the fig. 1, we

can write the corresponding electromagnetic current as :

$$J^{\mu}_{e.m.} = \bar{u}_{N^*}(p')[\frac{\bar{F}_2(q^2)i\sigma^{\mu\nu}q_{\nu}}{m+m^*} + \bar{F}_3(q^2)(q^{\mu} - \frac{q^2}{m^*-m}\gamma^{\mu})]u_N(p) \tag{7}$$

where $\bar{F}_{2,3}(q^2)$ are the electromagnetic form factors for the $N - N^*$ transition (which already include the proton charge), $q^{\mu} = (q^0, \vec{q})$ is the momentum of the virtual photon and the m, m^* the masses of the nucleon and the $N^*(1440)$ respectively. We can rewrite these form factors in terms of F_1, F_2, defined as: $F_1 = \frac{\bar{F}_3}{m^*-m}$ and $F_2 = \frac{\bar{F}_2}{m+m^*}$. The current of eq. (7) coincides with the one in [26] substituting there: $G_1 = -F_1$ and $G_2 = -\frac{2F_2}{m^*-m}$. We write our vertex functions as $V^{\mu}\epsilon_{\mu}$=$-iJ^{\mu}\epsilon_{\mu}$. By keeping terms up to (q/m) in a non relativistic reduction of the matrix elements of the Dirac gamma matrices we find:

$$V^{\mu}_{\gamma NN^*} = \left\{ \begin{array}{c} i\frac{\vec{q}^2}{2m}F_2(q^2) - i\vec{q}^{\,2}(1+\frac{q^0}{2m})F_1(q^2) \\ F_2(q^2)[i\vec{q}\,\frac{q^0}{2m} + (\vec{\sigma}\times\vec{q})(1+\frac{q^0}{2m})] - F_1(q^2)[i\vec{q}q^0(1+\frac{q^0}{2m}) + q^2\frac{1}{2m}(\vec{\sigma}\times\vec{q})] \end{array} \right\} \tag{8}$$

Next we construct the helicity amplitudes for our transition. There are many works where the helicity amplitudes are calculated [27, 32, 33, 34, 35]. In what follows we adjust to the formalism of ref. [27]. Then $A_{1/2}$ and $S_{1/2}$ can be written as:

$$A^{N^*}_{1/2} = \sqrt{\frac{2\pi\alpha}{q_R}}\frac{1}{e}\langle N^*, J_z = 1/2|\epsilon^{(+)}_{\mu}\cdot J^{\mu}|N, S_z = -1/2\rangle \tag{9}$$

$$S^{N^*}_{1/2} = \sqrt{\frac{2\pi\alpha}{q_R}}\frac{|\vec{q}|}{\sqrt{Q^2}}\frac{1}{e}\langle N^*, J_z = 1/2|\epsilon^{(0)}_{\mu}\cdot J^{\mu}|N, S_z = 1/2\rangle \tag{10}$$

where q_R is the energy of an equivalent real photon, $(W^2 - m^2)/(2W)$ and W is the photon-proton center of mass energy.

The tranverse polarization vectors are:

$$\epsilon^{(\pm)}_{\mu} = \frac{(0, \mp 1, -i, 0)}{\sqrt{2}} \tag{11}$$

and $\epsilon^0_{\mu} = \frac{1}{\sqrt{Q^2}}(q, 0, 0, q^0)$ normalized to unity, satisfying $\epsilon^0_{\mu}\cdot q^{\mu} = g^{\mu\nu}\epsilon^0_{\mu}\cdot\epsilon^{(\pm)}_{\nu} = 0$ with $\vec{q}$ in z direction and $Q^2 = -q^2$.

Using our electromagnetic current the helicity amplitudes are given by:

$$A^{N^*}_{1/2} = \sqrt{\frac{2\pi\alpha}{q_R}}\frac{1}{e}[F_2(q^2)\sqrt{2}q(1+\frac{q^0}{2m}) + F_1(q^2)Q^2\sqrt{2}\frac{q}{2m}] \tag{12}$$

and

$$S^{N^*}_{1/2} = \sqrt{\frac{2\pi\alpha}{q_R}}\frac{\vec{q}^{\,2}}{e}[-F_2(q^2)\frac{1}{2m} + F_1(q^2)(1+\frac{q^0}{2m})] \tag{13}$$

Inverting these equations we can get the electromagnetic form factors in terms of the helicity amplitudes. The experimental helicity amplitudes $A^p_{1/2}$ and $S^p_{1/2}$ which we use are taken from [36] which uses data from [37].

In the case of the $N^*(1520)$ resonance we can take the same steps as above. Following [26] we write the relativistic current as:

$$J^\mu_{e.m.} = G_1(q^2)J^\mu_1 + G_2(q^2)J^\mu_2 + G_3(q^2)J^\mu_3 \tag{14}$$

with

$$J^\mu_1 = \bar{u}_\beta(q^\beta\gamma^\mu - \not{q}g^{\beta\mu})u \tag{15}$$

$$J^\mu_2 = \bar{u}_\beta(q^\beta p'^\mu - p'\cdot q g^{\beta\mu})u \tag{16}$$

$$J^\mu_3 = \bar{u}_\beta(q^\beta q^\mu - q^2 g^{\beta\mu})u \tag{17}$$

and G_1,G_2,G_3 are the electromagnetic form factors for this vertex and p' is the momenta of the resonance.

Taking a non relativistic reduction as done before and using u_μ Rarita-Schwinger spinors in the c.m. of the resonance, the vertex takes an expression given by:

Scalar part:

$$V^0_{\gamma NN'^*} = i(G_1 + G_2 p'^0 + G_3 q^0)\vec{S}^\dagger\cdot\vec{q} \tag{18}$$

and the vector part:

$$\begin{aligned} V^i_{\gamma NN'^*} = -i[(\frac{G_1}{2m} - G_3)(\vec{S}^\dagger\cdot\vec{q})\,\vec{q} - \\ iG_1\frac{\vec{S}^\dagger\cdot\vec{q}}{2m}(\vec{\sigma}\times\vec{q}) - \vec{S}^\dagger\{G_1(q^0 + \frac{\vec{q}^{\,2}}{2m}) + G_2 p'^0 q^0 + G_3 q^2\}] \end{aligned} \tag{19}$$

Using again eqs.(9) and (10) we calculate the $A_{1/2}$ and $S_{1/2}$ helicity amplitudes for the $N^*(1520)$. In addition, in this case we also have the $A_{3/2}$ helicity amplitude which is given in [27] by:

$$A^{N^*}_{3/2} = \sqrt{\frac{2\pi\alpha}{q_R}}\frac{1}{e}\langle N^*, J_z = 3/2|\epsilon^{(+)}_\mu\cdot J^\mu|N, S_z = 1/2\rangle \tag{20}$$

The expressions for the helicity amplitudes obtained using the current in eqs.(14-17) are:

$$A^{N'^*}_{3/2} = \sqrt{\frac{2\pi\alpha}{q_R}}\frac{1}{e}[G_1(q^0 + \frac{\vec{q}^{\,2}}{2m}) + G_2 q^0 p'^0 + G_3 q^2] \tag{21}$$

$$A^{N'^*}_{1/2} = \sqrt{\frac{2\pi\alpha}{q_R}}\frac{1}{e}\frac{1}{\sqrt{3}}[G_1(q^0 - \frac{\vec{q}^{\,2}}{2m}) + G_2 q^0 p'^0 + G_3 q^2] \tag{22}$$

$$S_{1/2}^{N'*} = -\sqrt{\frac{2\pi\alpha}{q_R}}\frac{1}{e}\sqrt{\frac{2}{3}}q[G_1 + G_2 p'^0 + G_3 q^0] \tag{23}$$

From these three equations we can get the G_1, G_2, G_3 form factors in terms of the helicity amplitudes. The data for $S_{1/2}$ are taken from [27] and for $A_{1/2}$ and $A_{3/2}$ from [27, 38] [1].

The other important vertex in our model corresponds to the $\Delta - N$ electromagnetic transition. As discussed in [32, 33], the most important transition is the magnetic dipole (M_{1^+}) transition while the electric quadrupole (E_{1^+}) and scalar quadrupole (S_{1^+}) transitions are small at momentum transfers between the photon point to Q^2=1.3 GeV^2. The values given in [26] for the ratio E_{1^+}/M_{1^+} (S_{1^+}/M_{1^+}) are -0.02 to 0.02 (-0.025 to -0.06) for Q^2=0 to 1.3 GeV^2 respectively. We take the $\gamma N\Delta$ transition current from [39] where the same non relativistic expansion done here, keeping terms of order $O(p/m)$ for the Dirac matrix elements, is done. A good reproduction of the data for electroproduction of one pion was obtained there in a wide range of energies around the Δ resonance and different Q^2. The vertex for this electroproduction transition is given by eq. (40) in appendix A2 and the form factor used is given by eq. (61) in appendix A3.

4 Gauge invariance and form factors

Gauge invariance is one of the important elements in a model involving photons and implies that

$$T^\mu q_\mu = 0 \tag{24}$$

The explicit expressions for T^μ, keeping the four components, as given in appendix A4, allow one to check explicitly the gauge invariance. The block of diagrams D1, D2, D4 and D6 form together a gauge invariant set. The rest of the diagrams in which the photon directly excites a resonance from a nucleon are gauge invariant by themselves. However, some caution must be observed when imposing eq. (24). Indeed, in diagram D2 the intermediate pion is off-shell and induces a strong $\pi N\Delta$ transition form factor, $F_\pi(p^2)$, for which we take a usual monopole form factor (see eq.(53) appendix A3). The constraints of eq.(24) forces this form factor to appear in the other terms of the block of diagrams which are gauge invariant. However, as discussed in the study of the $eN \to e'N\pi$ reaction in [39], and as can be easily seen by inspection of the diagrams and the amplitudes, the constraint of eq. (24) still requires the equality of four electromagnetic form factors,

$$F_1^p(q^2) = F_1^\Delta(q^2) = F_{\gamma\pi\pi} = F_c(q^2) \tag{25}$$

[1] We note that the formalism followed here for the vertices of the $N^*(1520)$ is different from that of [2], but the same results are obtained for real photons.

The form factors of eq. (25), if the strict Feynmann rules of the appendix A4 are followed, are respectively the γNN, $\gamma\Delta\Delta$, $\gamma\pi\pi$ and $\gamma\Delta N\pi$ ones. These form factors are usually parametrized in different forms, as seen in appendix A3, except for $F_1^p(q^2)$ and $F_1^\Delta(q^2)$ which are taken equal, as it would come from ordinary quark models.

Although the model is gauge invariant with the prescription of eq. (25) there is the inconvenience that the results depend upon which one of the three form factors we take for all of them.

In the next section we discuss the uncertainties which come from this arbitrary choice of form factor. We should note however, that the dominant term, by large, is the Δ Kroll Ruderman and pion pole terms. This is also so in the test of gauge invariance where the two terms involving the $F_1^p(q^2)$ form factor in diagrams D4, D6 give only recoil contributions of the order of $\mathrm{O}(p_\pi/\mathrm{m})$ in eq. (24). This justifies the use of $F_c(q^2)$ or $F_{\gamma\pi\pi}(q^2)$ for all the form factors.

There is, however, another way to respect gauge invariance, while at the same time using different form factors which is proposed in [25] and to which we refer in what follows as Berends et al. approach. In the next section we will show the results from both approaches and will discuss them.

There are many papers in the literature following the Berends et al. approach in order to explain the experimental results with this gauge invariant set of diagrams [40, 41, 42, 43].

Another of the common approaches to this problem in the past has been the use of current algebra [44, 45, 46]. In this case, close to threshold of $\Delta\pi$ production, the axial vector current $\langle\Delta|A_\mu|N\rangle$ is the dominant term. In the soft pion limit this axial vector current is shown to be equivalent [45] to the one of the nucleon. The $\pi\Delta$ electroproduction data are hence used in those works to determine the nucleon axial form factor.

Our model is more general since one obtains explicit p_π^μ dependence, for instance from the pion pole term (diagram D.2 fig. 1). The dominance of the $\Delta N\pi\gamma$ Kroll Ruderman at threshold (independent of p_π^μ) offers however some support to the assumptions made in those works, as quoted in [30]. The diagrammatic approach relies however on the explicit use of the four form factors of eq. (25). We shall see in the next section the influence of the different terms close to threshold.

In [47], following the diagrammatic approach with the minimal set of gauge invariant terms, fits to the data are carried fixing $F_{\gamma\pi\pi}$ from ρ vector meson dominance and setting the other three form factors equal in order to determine this latter common form factor. A qualitative agreement with the $F_1^p(q^2)$ form factor obtained from others sources is found.

With the gauge invariant prescription of [25] using different form factors, different fits to the data are carried fixing some of the form factors and determining others. We shall follow this latter approach , but with our enlarged set of Feynman diagrams including the explicit decay of the Δ into πN, which allows one to keep track of correlations between the pions if wished. We will show the sensitivity of the results to different form factors and the weight of

the different terms as a function of energy and Q^2.

The explicit formulas of the gauge invariant set in the presence of the different form factors are taken from eq. (17) of ref. [25] and, after the non relativistic reduction is done, the expressions used here are shown in appendix A5.

5 Results and discussion

We have tested our results with the experimental data of refs. [22,30]. We show the cross section of $\gamma_v p \to \Delta^{++}\pi^-$ and $\gamma_v p \to \Delta^0\pi^+$ ($\Delta^0 \to \pi^- p$), as a function of W, the virtual photon-proton ($\gamma_v p$) center of mass energy, and for different values of Q^2. We have

$$W^2 = -Q^2 + M^2 + 2M\nu\,; \nu = E - E' \tag{26}$$

with

$$Q^2 = -q^2 = 4EE' sin^2(\frac{\theta_e}{2}) \tag{27}$$

We compare in fig. 2 the results for delta photoproduction (real photons) with the experimental data [48] and we see that the agreement found is quite satisfactory.

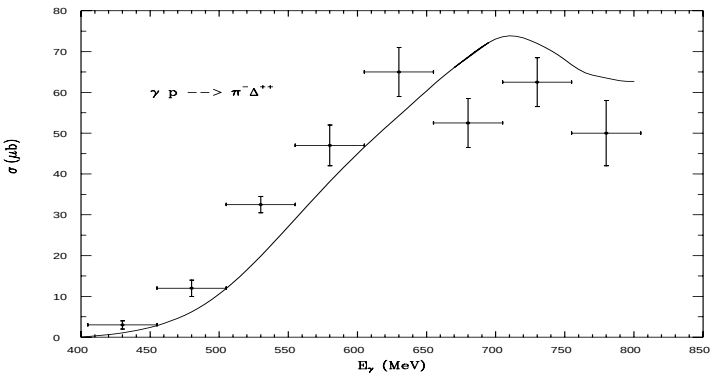

Figure 2: Cross section for the $\gamma p \to \Delta^{++}\pi^-$ reaction. Experimental data from [48].

In order to compare our results with experiment for virtual photons we calculate first the cross sections at $Q^2 = 0.6\ GeV^2$.

Figure 3 contains three different calculations. Two of them correspond to using all form factors equal (which we set to $F_{\gamma\pi\pi}$) with two different values of λ_π^2, 0.5 GeV^2 and 0.6 GeV^2. We see that the cross section increases by about 10 % when going from λ_π^2=0.5 GeV^2 and λ_π^2=0.6 GeV^2. We also show the results taking F_1^p, F_1^Δ with their values given in appendix A3 and setting $F_c = F_{\gamma\pi\pi}$ with λ_π^2=0.6 GeV^2. This latter calculation is not gauge invariant.

However we see that the deviation with respect to the gauge invariant one assuming all form factors equal is very small. This reflects the fact that the relevant terms in the model are those involving $F_{\gamma\pi\pi}$ and F_c, the pion pole and Δ Kroll Ruderman terms.

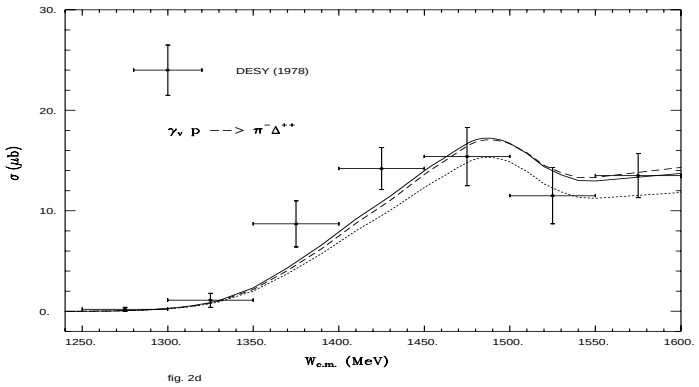

Figure 3: Cross section for $\gamma_v p \to \pi^- \Delta^{++}$ as a function of the $\gamma_v p$ center of mass energy. The curves correspond to $Q^2 = 0.6\ GeV^2$. Dashed line: F_1^p, F_1^Δ, from appendix A3 and F_c=$F_{\gamma\pi\pi}$ with $\lambda_\pi^2 = 0.6\ GeV^2$. Continuous line: $F_1^p = F_1^\Delta = F_c = F_{\gamma\pi\pi}$ with $\lambda_\pi^2 = 0.6\ GeV^2$. Dotted line: same as continuous line with $\lambda_\pi^2 = 0.5\ GeV^2$

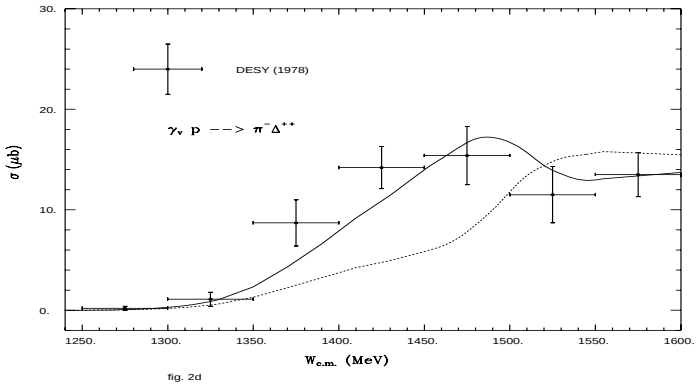

Figure 4: Continuous line: Cross section for $\gamma_v p \to \pi^- \Delta^{++}$ at Q^2= 0.6 GeV^2 using $F_1^p = F_1^\Delta = F_{\gamma\pi\pi} = F_c$ with λ_π^2=0.6 GeV^2 and $\tilde{f}_{N^{*\prime}\Delta\pi} = -0.911$, $\tilde{g}_{N^{*\prime}\Delta\pi}$=0.552. Dotted line: same as continuous line but with $\tilde{f}_{N^{*\prime}\Delta\pi}$=0.911 and $\tilde{g}_{N^{*\prime}\Delta\pi} = -0.552$. See appendices A1 and A2 for the vertices and coupling constants used.

In refs. [2,14], two solutions for the coupling of the $N^*(1520)$ to the Δ in s and $d-waves$, differring only in a global sign, were found from the respective decay widths. Only a sign was compatible with the experimental $(\gamma, \pi\pi)$ data, because of the strong interference between the $\gamma N \to N^*(1520) \to \Delta\pi$ term and the Kroll Rudermam one. Here, in the new formalism the amplitude of the $\gamma N \to N^*(1520)$ transition changes sign and consequently the signs of the former $N^*(1520) \to \Delta\pi$ couplings must be changed. In fig. 4 we show the results of $\gamma_v p \to \pi^- \Delta^{++}$ at Q^2=0.6 GeV^2 using the two different signs for these

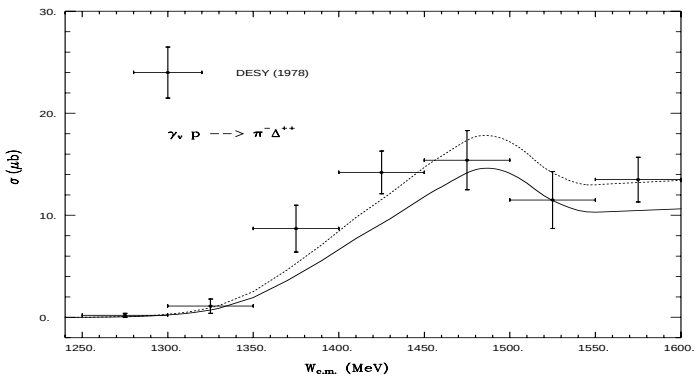

Figure 5: Cross sections from $\gamma_v p \to \Delta^{++}\pi^-$ with Berends formalism included. Continuous line: $F_1^p, F_1^\Delta, F_{\gamma\pi\pi} = F_c$ with $\lambda_\pi^2 = 0.5\ GeV^2$. Dotted line: same as continuous line with the parameter for $F_{\gamma\pi\pi}$ 0.5 GeV^2 and for F_c is 0.8 GeV^2.

couplings. We can see that the data favour clearly one of the signs. This was also observed in the $\gamma p \to \pi^+\pi^- p$ reaction in [14]. Fig. 4 shows the magnitude of the interference between those terms. Neglecting the $\gamma p \to N^*(1520) \to \Delta\pi$ process leads to results in between the two curves shown in the figure where one does not see any peak. The peak shown by the data around W=1480 MeV is hence not reminiscent of a Δ but a peak coming from the constructive interference of the terms mentioned above.

Now we evaluate the cross section using Berends gauge invariant approach with different form factors [25] using the formulae of appendix A5 for the set of the four gauge invariant terms. We show the results in fig. 5. The continuous line in the figure is obtained with this prescription using the form factors of appendix A3 for the F_1^p, F_1^Δ but setting $F_c = F_{\gamma\pi\pi}$ with $\lambda_\pi^2 = 0.5\ GeV^2$.

We can see that these results are remarkably similar to those of the dotted line in fig. 3 where F_c and $F_{\gamma\pi\pi}$ had the same values as here but F_1^p, F_1^Δ were set equal to $F_{\gamma\pi\pi}$ in order to preserve gauge invariance.

Once again we can see that the terms involving F_1^p and F_1^Δ are relatively unimportant, or in any case that setting these form factors equal to $F_{\gamma\pi\pi}$ provide a gauge invariant result very close to the one obtained with the more general Berends prescription of [25].

The dotted line in fig. 5 corresponds to the same parametrization for F_c as for $F_{\gamma\pi\pi}$ but parameter λ_c^2= 0.8 GeV^2. This shows the sensitivity of the results to F_c which appears in the dominant Kroll-Ruderman term.

Given the dominance of the Kroll Ruderman term close to threshold production of $\Delta\pi$ in our model and the dominance of the terms involving the axial form factor in the current algebra approaches, we now show in fig. 6 the results taking for F_c the parametrization of the axial vector form factor (see appendix A3), varying the value of M_A. The Berends formalism with different form factors is used, and F_1^p, F_1^Δ, $F_{\gamma\pi\pi}$ are taken as in appendix A3. We can see that the experimental data favour values of $M_A \simeq$ 1.16-1.23 GeV very similar to the values determined in [30] (1.16± 0.03) GeV or [44] (1.18± 0.07)

GeV.

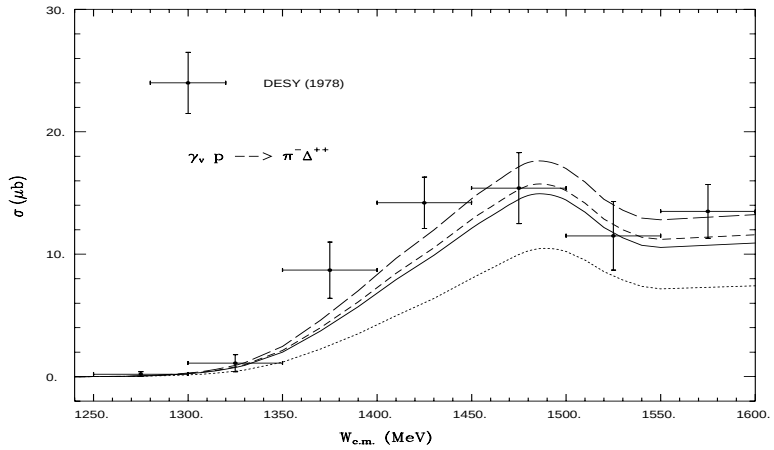

Figure 6: Cross sections for $\gamma_v p \to \pi^- \Delta^{++}$ within Berends formalism. We use different form factors for F_1^p, F_1^Δ, $F_{\gamma\pi\pi}$ from appendix A3. We take for the axial form factor, F_A, form the contact term. The parameter M_A is changed from up to down :1.32, 1.23, 1.16, 0.89 in GeV.

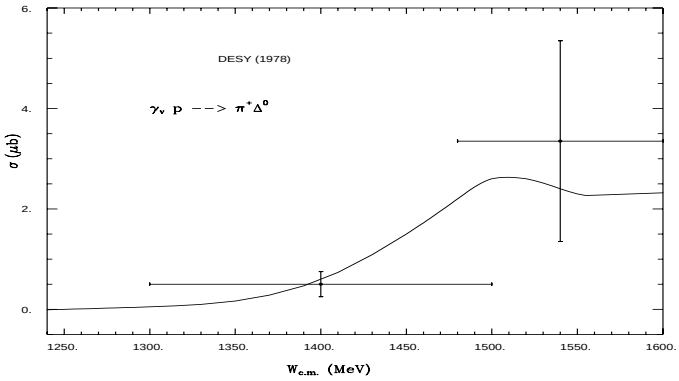

Figure 7: Cross section for $\gamma_v p \to \pi^+ \Delta^0$ within Berends formalism. We use $F_1^p, F_1^\Delta, F_{\gamma\pi\pi}$ from appendix A3 and F_A with M_A=1.16 GeV.

In fig. 7 we show the cross section for $\gamma_v p \to \Delta^0 \pi^+$ with Berends scheme and with a value of the axial form factor parameter of $M_A = 1.16$ GeV. We find a good agreement with the scarce experimental data but more data would be required to further check this channel.

In all these sets of figures for Δ^{++} electroproduction we find a good agreement with the experimental results around the peak region 1460 MeV$\leq$ W $\leq$ 1600 MeV in c.m. energy at Q^2=0.6 GeV^2. As commented above, this peak comes from the interference between the Δ Kroll Ruderman and the $N^*(1520)$ excitation terms, which was also found for real photons in [1,2,14]. A priori this interference pattern could change for virtual photons since these two terms are affected by different form factors, $F_c(q^2)$ for the contact term and the form

factors $G_1(q^2), G_2(q^2), G_3(q^2)$ that appear for the $\gamma N \to N^*(1520)$ transition. In practice we see that the interference survives in the case of virtual photons.

The $N^*(1520)$ excitation has a longitudinal coupling and so has the Δ. The inclusion of this longitudinal contribution could also blur the interference found with these two terms for real photons. However, the results shown for virtual photons show that the interference remains also in this latter case. We have checked that if we go up to higher Q^2 the interference still exists but the shape becomes flatter.

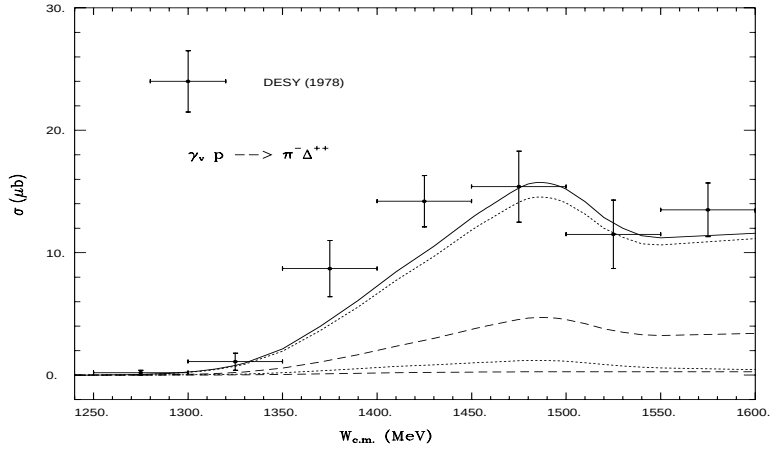

Figure 8: Continuous line: cross section for $\gamma_v p \to \Delta^{++}\pi^-$ within Berends formalism and with the parameter M_A=1.23 GeV at Q^2=0.6 GeV^2. Dotted lines: From up to down we show the tranverse σ_T and longitudinal $\epsilon\sigma_L$ cross section at Q^2=0.6 GeV^2 respectively. Short-dashed lines: From up to down the same as in dotted line for Q^2=1.2 GeV^2.

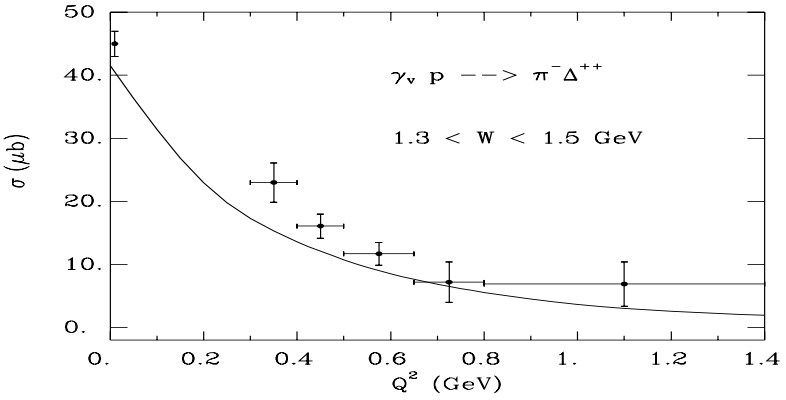

Figure 9: Cross section $\gamma_v p \to \Delta^{++}\pi^-$ as a function of the Q^2.

It is interesting to show separate contributions for the longitudinal and transverse cross sections which are likely to be also measured at TJNAF. We

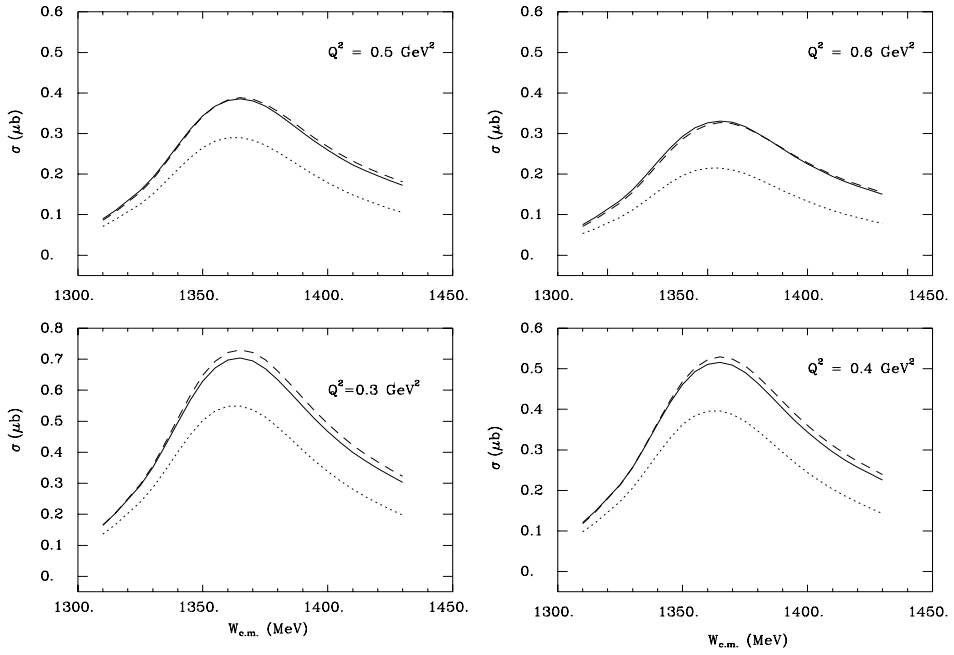

Figure 10: Continuous line: Total cross section from $\gamma_v \to \pi^- \Delta^{++}$ within Berens formalism restricting $m_\pi \leq \omega_{\pi^-} \leq m_\pi + 10$ MeV. We use F_1^p, F_1^Δ from appendix A3 and $F_{\gamma\pi\pi}$ with $\lambda_\pi^2 = 0.5\ GeV^2$. Dotted lined: Contribution of Δ Kroll Ruderman term using F_A with M_A=1.16 GeV. Short-dashed line: Contribution of Δ Kroll Ruderman term plus the interference with the $N^*(1520)$ term.

.

find in fig. 8 that the shape of the curves for the transverse contribution is the same as for real photons and for the sum of the longitudinal and transverse cross sections for the virtual ones. We observe that the longitudinal contribution gives only a small background. This pattern appears for any intermediate values of Q^2 between those shown in the figure.

In fig. 9 we show a cross section as a function of the momentum transfer Q^2 and we compare with the experimental data from [22,30].

We have made an average of the cross sections between 1300 to 1500 MeV c.m. energy in order to compare with the experiment. We observe that the trend of the data is well reproduced, but the absolute value is a little lower reflecting the discrepances with the data in fig. 8 in that range of energies.

In fig. 10 we show some results which can be a guideline for an experimental analysis. We concentrate on a hypothetical measurement that strengtens the contribution of the Kroll Ruderman term in order to optimize the chances to obtain an accurate value for the contact form factor $F_c(q^2)$. This can be accomplished by fixing the energy of the π^- and hence putting the Δ^{++} on shell in the diagram D.1 of fig. 1. In fig. 10 we take $m_\pi \leq \omega_{\pi^-} \leq m_\pi + 10$ MeV and show the results obtained for different Q^2 selecting the Kroll Ruderman term alone, this term plus the interference with the $N^*(1520)$ and the total

contribution. We see indeed that this magnitude is largely dominated by the Kroll Ruderman term. However the interference with the $N^*(1520)$ term is always present. Since the weight of the $N^*(1520)$ propagator is smaller at lower energies, we can also see that the region to the left of the Δ peak which appears in the figure is more suited to pin down the contribution of the Kroll Ruderman term. Yet, even at this lower energies the contribution of the interference term is still of the order of 20 per cent. This means that the accurate evaluation of $F_c(q^2)$ at level better than 20 per cent requires a careful analysis in which the interference term is explicitly considered.

6 Conclusions

We have calculated cross sections for the $\gamma_v p \to \Delta^{++}\pi^-$ and $\gamma_v p \to \Delta^0\pi^+$ reactions, extending the model of ref. [2] to virtual photons and selecting the diagrams which have a Δ in the final state.

The present calculations and comparison with the scarce experimental data are sufficient to establish the fairness of the present model to deal with the $\Delta\pi$ production process. In summary we could remark the following points:

Even if the data are scarce the agreement with them is good up to W$\simeq$ 1.6 GeV and $Q^2 \simeq 1.4\ GeV^2$ for the Δ^{++} channel. However, it would be desirable to have data for different values of Q^2. In the future such experiments are bound to be made in Thomas Jefferson Laboratory and other experimental facilities. Also other channels should be measured as well as total cross sections for $\gamma_v N \to \pi\pi N$ where the πN are not in a Δ state.

We have also shown that the peak in the cross section is due to an interference between the Δ Kroll Ruderman term and the $N^*(1520)$ excitation process followed by $\Delta\pi$ decay. This interference appeared in real photons and is not destroyed for virtual ones in spite of the fact that the electromagnetic form factors of the respective mechanisms are not exactly the same. In addition, the contribution from the longitudinal couplings in the terms involved in the interference does not destroy this effect. The experiments show clearly that interference of the two mechanisms is contructive below the $N^*(1520)$ pole, which is consistent with the findings in real photons and predictions of the relativized quark models.

Different sets of form factors have been used in our model in order to show the sensitivity of the results to these changes. These tests should be useful in view of the coming data and the possibility to extract relevant information from them.

Some plots can be useful for the experimental task. We have shown the separation of the transverse and longitudinal cross sections and found that the transverse one largely dominates the cross sections.

We have also shown a method aimed at obtaining the form factor for the Kroll Ruderman term selecting a kinematics which maximizes its importance. Even then we saw that an accurate extraction of this form factor requires the

explicit inclusion of the $N^*(1520)$ term in the analysis because of the important interference of this term with the Kroll Ruderman one.

Finally, it is also interesting to note that the present model is just part of a more general $\gamma_v N \to \pi\pi N$ model which selects only the terms where a πN pair of the final state appears forming a Δ state. Both experiments and theoretical calculations on the different $(\gamma_v, \pi\pi)$ channels should be encouraged.

Acknowledgements. We would like to thank J.A. Gómez-Tejedor, F. Cano and L. Alvarez-Ruso for useful discussions. We would like to acknowledge partial financial support for DGICYT contract number PB96-0753. One of us, J.C.N. would like to acknowledge the support from the Ministerio de Educacion y Cultura.

APPENDIX

A1. Lagrangians.

$$L_{\pi NN} = -\frac{f}{\mu}\overline{\Psi}\gamma^{\mu}\gamma_5\partial_{\mu}\vec{\phi}\cdot\vec{\tau}\Psi \tag{28}$$

$$L_{\Delta\pi N} = -\frac{f^*}{\mu}\Psi^{\dagger}_{\Delta}S^{\dagger}_i(\partial_i\phi^{\lambda})T^{\lambda\dagger}\Psi_N + h.c. \tag{29}$$

$$L_{\Delta\Delta\pi} = -\frac{f_{\Delta}}{\mu}\Psi^{\dagger}_{\Delta}S_{\Delta i}(\partial_i\phi^{\lambda})T^{\lambda}_{\Delta}\Psi_{\Delta} + h.c. \tag{30}$$

$$L_{N^*\Delta\pi} = -\frac{g_{N^*\Delta\pi}}{\mu}\Psi^{\dagger}_{\Delta}S^{\dagger}_i(\partial_i\phi^{\lambda})T^{\lambda\dagger}\Psi_{N^*} + h.c. \tag{31}$$

$$L_{N^{*\prime}\Delta\pi} = i\overline{\Psi}_{N^{*\prime}}(\tilde{f}_{N^{*\prime}\Delta\pi} - \frac{\tilde{g}_{N^{*\prime}\Delta\pi}}{\mu^2}S^{\dagger}_i\partial_i S_j\partial_j)\phi^{\lambda}T^{\lambda\dagger}\Psi_{\Delta} + h.c. \tag{32}$$

$$L_{NN\gamma} = -e\overline{\Psi}_N(\gamma^{\mu}A_{\mu} - \frac{\chi_N}{2m}\sigma^{\mu\nu}\partial_{\nu}A_{\mu})\Psi_N \tag{33}$$

$$L_{\pi\pi\gamma} = ie(\phi_+\partial^{\mu}\phi_- - \phi_-\partial^{\mu}\phi_+)A_{\mu} \tag{34}$$

Instead of writing the explicit expressions for the terms involving the photon and the excitation of resonances like $L_{\Delta N\gamma}$, $L_{N^*N\gamma}$, $L_{\Delta\pi\gamma N}$ and $L_{N^{*\prime}N\gamma}$, we address the reader directly to eqs. (40, 43-44, 50, 51-52) respectively which provide the vertex function ($L \to -V^{\mu}\epsilon_{\mu}$).

In the former expressions $\vec{\phi}$, Ψ, Ψ_{Δ}, Ψ_{N^*}, $\Psi_{N^{\prime *}}$ and A_{μ} stand for the pion, nucleon, Δ, N^*, $N^{\prime *}$ and photon fields, respectively ; N^* and $N^{\prime *}$ stand for the $N^*(1440)$ and $N^*(1520)$; resonances m and μ are the nucleon and the pion masses; $\vec{\sigma}$ and $\vec{\tau}$ are the spin and isospin 1/2 operators; $\vec{S^{\dagger}}$ and $\vec{T^{\dagger}}$ are the transition spin and isospin operators from 1/2 to 3/2 with the normalization

$$\langle\frac{3}{2}, M|S^{\dagger}_{\nu}|\frac{1}{2}, m\rangle = C(\frac{1}{2}, 1, \frac{3}{2}; m, \nu, M) \tag{35}$$

with ν in spherical base, and the same for $T^{\dagger}$. The operators $\vec{S}_{\Delta}$ and $\vec{T}_{\Delta}$ are the ordinary spin and isospin matrices for the a spin and isospin 3/2 object. For the pion fields we used the Bjorken and Drell convention :

$$\phi_+ = \frac{1}{\sqrt{2}}(\phi_1 - i\phi_2) \quad destroys \quad \pi^+, creates \quad \pi^- \tag{36}$$

$$\phi_- = \frac{1}{\sqrt{2}}(\phi_1 + i\phi_2) \quad destroys \quad \pi^-, creates \quad \pi^+ \tag{37}$$

$$\phi_0 = \phi_3 \quad destroys \quad \pi^0, creates \quad \pi^0 \tag{38}$$

Hence the $|\pi^+\rangle$ state corresponds to $-|11\rangle$ in isospin base.
In all formulae we have assumed that $\sigma^i \equiv \sigma_i$, $S^i \equiv S_i$, $T^i \equiv T_i$ are Euclidean vectors. However for ∂_i, A_i, p_i, etc, we have respected their covariant meaning.

A2. Feynman Rules.

Here we write the Feynman rules for the different vertices including already the electromagnetic form factors. We assumed the photon with momenta q as an incoming particle while the pion with momentum k is an outgoing particle in all vertices. The momentum p, p' are those of the baryonic states just before and after the photon absorption vertex (or pion production vertex in eq. (42)).

$$V^{\mu}_{\gamma NN} = -ie \left\{ \begin{array}{c} F_1^N(q^2) \\ F_1^N(q^2)[\frac{\vec{p}+\vec{p}'}{2m}] + i\frac{\vec{\sigma}\times\vec{q}}{2m} G_M^N(q^2) \end{array} \right\} \tag{39}$$

$$V^{\mu}_{\gamma N\Delta} = \sqrt{\frac{2}{3}} \frac{f_\gamma(q^2)}{m_\pi} \frac{\sqrt{s}}{m_\Delta} \left\{ \begin{array}{c} \frac{\vec{p}_\Delta}{\sqrt{s}}(\vec{S^\dagger} \times \vec{q}) \\ \frac{p^0_\Delta}{\sqrt{s}}[\vec{S^\dagger} \times (\vec{q} - \frac{q^0}{p^0_\Delta}\vec{p_\Delta})] \end{array} \right\} \tag{40}$$

$$V_{\pi N\Delta} = -\frac{f^*}{\mu} \vec{S^\dagger} \cdot (\vec{k} - \frac{k^0}{\sqrt{s}}\vec{p_\Delta}) T^{\lambda\dagger} \tag{41}$$

$$V_{\pi NN} = -\frac{f}{\mu}(\vec{\sigma}\vec{k} - k^0 \frac{\vec{\sigma}(\vec{p}+\vec{p}')}{2m})\tau^\lambda \tag{42}$$

$$V^0_{N^*N\gamma} = i\frac{\vec{q}^{\,2}}{2m} F_2(q^2) - i\vec{q}^{\,2}(1 + \frac{q^0}{2m}) F_1(q^2) \tag{43}$$

$$\begin{aligned} V^i_{N^*N\gamma} = {} & F_2(q^2)[i\vec{q}\frac{q^0}{2m} + (\vec{\sigma}\times\vec{q})(1+\frac{q^0}{2m})] \\ & -F_1(q^2)[i\vec{q}q^0(1+\frac{q^0}{2m}) + q^2\frac{1}{2m}(\vec{\sigma}\times\vec{q})] \end{aligned} \tag{44}$$

$$V_{N^*\Delta\pi} = -\frac{g_{N^*\Delta\pi}}{\mu} \vec{S^\dagger} \cdot \vec{k} T^{\lambda\dagger} \tag{45}$$

$$V_{\Delta\Delta\pi} = -\frac{f_\Delta}{\mu} \vec{S_\Delta} \cdot \vec{k}\, T^\lambda_\Delta \tag{46}$$

$$V_{N^{*\prime}\Delta\pi} = -(\tilde{f}_{N^{*\prime}\Delta\pi} + \frac{\tilde{g}_{N^{*\prime}\Delta\pi}}{\mu^2} \vec{S^\dagger} \cdot \vec{k} \vec{S} \cdot \vec{k}) T^{\lambda\dagger} \tag{47}$$

$$V^{\mu}_{\gamma\Delta\Delta} = -i \left\{ \begin{array}{c} e_\Delta F_1^\Delta(q^2) \\ e_\Delta F_1^\Delta(q^2)[\frac{\vec{p}+\vec{p'}}{2m_\Delta}] + i\frac{\vec{S_\Delta}\times\vec{q}}{3m} e G_M^\Delta(q^2) \end{array} \right\} \tag{48}$$

$$V^{\mu}_{\pi\pi\gamma} = -iq_\pi(k^\mu + k'^\mu) F_{\gamma\pi\pi}(q^2) \tag{49}$$

$$V^{\mu}_{\Delta N\gamma\pi} = -q_{\pi}\frac{f^*}{m_{\pi}}T^{\lambda\dagger}\left\{\begin{array}{c}\vec{S}^{\dagger}\,\frac{\vec{p}_{\Delta}}{\sqrt{s}}\\ \vec{S}^{\dagger}\end{array}\right\}F_c(q^2) \tag{50}$$

$$V^{0}_{\gamma NN'^*} = i(G_1(q^2) + G_2(q^2)p'^0 + G_3(q^2)q^0)\vec{S}^{\dagger}\cdot\vec{q} \tag{51}$$

$$\begin{aligned} V^{i}_{\gamma NN'^*} = -i[(\frac{G_1(q^2)}{2m} - G_3(q^2))(\vec{S}^{\dagger}\cdot\vec{q})\,\vec{q} - iG_1(q^2)\frac{\vec{S}^{\dagger}\cdot\vec{q}}{2m}(\vec{\sigma}\times\vec{q}) \\ -\vec{S}^{\dagger}\{G_1(q^2)(q^0 + \frac{\vec{q}^{\,2}}{2m}) + G_2(q^2)p'^0q^0 + G_3(q^2)q^2\}] \end{aligned} \tag{52}$$

A3. Coupling and form factors

Coupling constants :

$f = 1 \qquad f^* = 2.13$

$f_{\Delta N\gamma} = 0.122 \qquad f_\Delta = 0.802$

$e = 0.3027$

$\tilde{f}_{N^{*\prime}\Delta\pi} = -0.911 \qquad \tilde{g}_{N^{*\prime}\Delta\pi} = 0.552$

$g_{N^*\Delta\pi} = 2.07$

Form factors :

For the off-shell pions we use a form factor of the monopole type :

$$F_\pi(p^2) = \frac{\Lambda_\pi^2 - \mu^2}{\Lambda_\pi^2 - p^2} \qquad ; \Lambda_\pi \sim 1250\, MeV \tag{53}$$

The Sachs's form factors are given by

$$G_M^N(q^2) = \frac{\mu_N}{(1 - \frac{q^2}{\Lambda^2})^2} \qquad ; G_E^N(q^2) = \frac{1}{(1 - \frac{q^2}{\Lambda^2})^2} \tag{54}$$

with $\Lambda^2 = 0.71\ GeV^2$; $\mu_p = 2.793$; $\mu_n = -1.913$.

The relation between $F_1^p(q^2)$ (Dirac's form factor) and $G_E^p(q^2)$ is :

$$F_1^p(q^2) = G_E^p(q^2)\frac{(1 - \frac{q^2\mu_p}{4m_N^2})}{(1 - \frac{q^2}{4m_N^2})} \tag{55}$$

and $F_1^n = 0$.

For the delta resonance we use

$$F_1^\Delta = F_1^p(q^2) \tag{56}$$

$$G_M^\Delta(q^2) = \frac{\mu_\Delta}{(1 - \frac{q^2}{\Lambda^2})^2} \tag{57}$$

In the case of the Δ^{++} we make use of the experimental value $\mu_{\Delta^{++}} = 1.62$ μ_p and for the other charge states we make use of the ratio ($e > 0$):

$$\frac{\mu_\Delta}{\mu_p} = \frac{e_\Delta}{e} \tag{58}$$

For the $\gamma\pi\pi$ vertex in diagram D2, we take the form factor:

$$F_{\gamma\pi\pi}(q^2) = \frac{1}{(1 - \frac{q^2}{\lambda_\pi^2})} \tag{59}$$

with $\lambda_\pi^2 = 0.5\ GeV^2$.

The axial nucleon form factor is given by:

$$F_A(q^2) = \frac{1}{(1 - \frac{q^2}{M_A^2})^2} \tag{60}$$

with $M_A = 1.16$ GeV. This form factor is used for the contact form factor, $F_c(q^2)$, in some of the results reported here. Some others results use $F_c(q^2) = F_{\gamma\pi\pi}(q^2)$.

The form factor for the $\gamma\Delta N$ transition is taken as:

$$f_\gamma(q^2) = f_\gamma(0) \frac{(1 - \frac{q^2}{(m_\Delta + m)^2})}{(1 - \frac{q^2 \mu_p}{4m_N^2})} \frac{G_M^p(q^2)}{\mu_p} \frac{(m_\Delta + m)^2}{(m_\Delta + m)^2 - q^2} \tag{61}$$

where $f_\gamma(0) = 0.122$

A4. Amplitudes for the reaction

In this appendix we write the explicit expressions for the amplitudes of the Feynman diagrams used in the model. The isospin coefficients and some constant factors are collected in the coefficients C which are written in the table A4.

Reaction	D1	D2	D3	D4	D5	D6	D7	D8
$\gamma_v p \to \pi^- \Delta^{++}$	-i/3	-i/3	0	i/3	1	i/3	i	-1
$\gamma_v p \to \pi^+ \Delta^0$	i/9	i/9	-2i/9	i/9	-2/3	0	i/3	-1/3

Table A4: Coefficients of the amplitudes for the Δ^{++} and Δ^0 ($\Delta^0 \to \pi^- p$) reactions, accounting for isospin and constant factors.

In the following expressions q, p_1, p_2, p_4, and p_5 are the momentum of the photon,the incoming nucleon, the outgoing nucleon and the two pions :

γ	p	π^+	π^-	p
q	p_1	p_5	p_4	p_2

We write only the amplitude when the pion labelled p_5 is emitted before the pion labelled p_4(Δ^0 case), except in the case of the D6 where the only

possibility is the Δ^{++} and the explicit amplitude for this case is written. We have also evaluated the crossed diagrams when the pion labelled p_5 is emitted after the pion called $p_4(\Delta^{++}$ case). Such amplitudes are exactly the same than the others written before, but exchanging the momenta p_4 and p_5 and changing some isospin coefficient. This latter change is taken into account by the factor C written in table A4.

We should note that in the vertex $\Delta N\pi$, when $\vec{p}_\Delta$ is not zero, we must change $\vec{p}_\pi$ by $\vec{p}_\pi - \frac{p^0}{\sqrt{s}}\vec{p}_\Delta$ for the final pion.

In the formulae, D_π, G_Δ, G_N, G_{N^*}, $G_{N'^*}$ are the propagator of the pion, delta, nucleon, $N^*(1440)$, $N^*(1520)$ respectively. Expressions for them and for the width of the resonances can be found in [1, 2, 14].

$$
\begin{aligned}
-iT_1^\mu &= Ce(\frac{f^*}{\mu})^2 G_\Delta(p_2+p_4)F_\pi((p_5-q)^2)F_c(q^2) \\
&\times \left\{ \begin{array}{c} [2\vec{p}_4\cdot\vec{p}_5 - i(\vec{p}_4\times\vec{p}_5)\cdot\vec{\sigma}]\frac{-1}{\sqrt{s_\Delta}} \\ 2\vec{p}_4 - i(\vec{\sigma}\times\vec{p}_4) \end{array} \right\}
\end{aligned} \tag{62}
$$

$$
\begin{aligned}
-iT_2^\mu &= Ce(\frac{f^*}{\mu})^2 G_\Delta(p_2+p_4)D_\pi(p_5-q)F_\pi((p_5-q)^2)F_{\gamma\pi\pi}(q^2) \\
&\times[2\vec{p}_4\cdot(\vec{p}_5-\vec{q}) - i(\vec{p}_4\times(\vec{p}_5-\vec{q}))\cdot\vec{\sigma}] \\
&\times \left\{ \begin{array}{c} 2p_5 - q \end{array} \right\}^\mu
\end{aligned} \tag{63}
$$

$$
\begin{aligned}
-iT_3^\mu &= C\frac{f}{\mu}\frac{f^*}{\mu}\frac{f_\gamma(q^2)}{\mu}G_N(p_2+p_4)G_\Delta(p_1+q) \\
&\times \left\{ \begin{array}{c} [-2i(\vec{p}_4\times\vec{q}) - (\vec{\sigma}\cdot\vec{q})\vec{p}_4 + (\vec{p}_4\cdot\vec{q})\vec{\sigma}]\frac{\vec{p}_\Delta}{m_\Delta} \\ [-2i(\vec{p}_4\times\vec{q}') - (\vec{\sigma}\cdot\vec{q}')\vec{p}_4 + (\vec{p}_4\cdot\vec{q}')\vec{\sigma}]\frac{p^0_\Delta}{m_\Delta} \end{array} \right\} \\
&\times[-p_5^0\frac{\vec{\sigma}(2\vec{p}_1-\vec{p}_5)}{2m} + \vec{\sigma}\vec{p_5}]
\end{aligned} \tag{64}
$$

with $\vec{q}' = (\vec{q} - \frac{q^0}{p^0_\Delta}\vec{p_\Delta})$

$$
\begin{aligned}
-iT_4^\mu &= Ce(\frac{f^*}{\mu})^2 G_N(p_1+k)G_\Delta(p_2+p_4)F_\pi((p_5-q)^2) \\
&\times[2\vec{p}_4\cdot\vec{p}_5 - i(\vec{p}_4\times\vec{p}_5)\cdot\vec{\sigma}] \\
&\times \left\{ \begin{array}{c} F_1^p(q^2) \\ F_1^p(q^2)[\frac{\vec{p}+\vec{p}'}{2m}] + iG_M^p(q^2)\frac{\vec{\sigma}\times\vec{q}}{2m} \end{array} \right\}
\end{aligned} \tag{65}
$$

$$
-iT_5^0 = 0 \quad in \quad \gamma - p \quad CM \quad frame \tag{66}
$$

$$
\begin{aligned}
-iT_5^i &= C\frac{f^*}{\mu}\frac{f_\Delta}{\mu}\frac{f_\gamma(q^2)}{\mu}G_\Delta(p_2+p_4)G_\Delta(p_1+q) \\
&\times[i\frac{5}{6}(\vec{p}_4\cdot\vec{q})\vec{p}_5 - i\frac{5}{6}(\vec{p}_5\cdot\vec{q})\vec{p}_4 - \frac{1}{6}(\vec{p}_4\cdot\vec{p}_5)(\vec{\sigma}\times\vec{q}) - \\
&\frac{1}{6}(\vec{p}_4\cdot\vec{\sigma})(\vec{p}_5\times\vec{q}) + \frac{2}{3}(\vec{p}_5\cdot\vec{\sigma})(\vec{p}_4\times\vec{q})]
\end{aligned} \tag{67}
$$

$$
\begin{aligned}
-iT_6^0 &= C(\frac{f^*}{\mu})^2 G_\Delta(p_2+p_5)G_\Delta(p_1-p_4)F_\pi((p_5-q)^2)\{e_\Delta F_1^\Delta(q^2) \\
&\times[2\vec{p}_5\cdot\vec{p}_4 - i(\vec{p}_5\times\vec{p}_4)\cdot\vec{\sigma}]\}
\end{aligned} \tag{68}
$$

$$
\begin{aligned}
-iT_6^i &= C(\frac{f^*}{\mu})^2 G_\Delta(p_2+p_5)G_\Delta(p_1-p_4)F_\pi((p_5-q)^2) \\
&\times\{\frac{e_\Delta F_1^\Delta(q^2)}{2}\frac{(\vec{p}_1-2\vec{p}_4)}{m_\Delta}[2\vec{p}_5\cdot\vec{p}_4 - i(\vec{p}_5\times\vec{p}_4)\cdot\vec{\sigma}] + \\
&i\frac{eG_M^\Delta(q^2)}{m}[i\frac{5}{6}(\vec{p}_4\cdot\vec{q})\vec{p}_5 - i\frac{5}{6}(\vec{p}_5\cdot\vec{q})\vec{p}_4 - \frac{1}{6}(\vec{p}_5\times\vec{q})(\vec{p}_4\cdot\vec{\sigma}) - \\
&\frac{1}{6}(\vec{p}_5\cdot\vec{\sigma})(\vec{p}_4\times\vec{q}) + \frac{2}{3}(\vec{p}_5\cdot\vec{p}_4)(\vec{\sigma}\times\vec{q})]\}
\end{aligned} \tag{69}
$$

Amplitude of N'^*(1520):
Vector part :

$$
\begin{aligned}
-iT_7^i &= C\frac{f^*}{\mu}G_\Delta(p_2+p_4)G_{N'^*}(p_1+q) \\
&\times\vec{S}\cdot\vec{p}_4[\tilde{f}_{N'^*\Delta\pi} + \frac{\tilde{g}_{N'^*\Delta\pi}}{\mu^2}\vec{S}^\dagger\cdot\vec{p}_5\vec{S}\cdot\vec{p}_5] \\
&\times\{(\frac{G_1(q^2)}{2m} - G_3(q^2))(\vec{S}^\dagger\cdot\vec{q})\,\vec{q} - iG_1(q^2)\frac{\vec{S}^\dagger\cdot\vec{q}}{2m}(\vec{\sigma}\times\vec{q}) \\
&-\vec{S}^\dagger[G_1(q^2)(q^0+\frac{\vec{q}^2}{2m}) + G_2(q^2)p'^0q^0 + G_3(q^2)q^2]\}
\end{aligned} \tag{70}
$$

scalar part:

$$
\begin{aligned}
-iT_7^0 &= -C\frac{f^*}{\mu}G_\Delta(p_2+p_4)G_{N'^*}(p_1+q) \\
&\times\vec{S}\cdot\vec{p}_4[\tilde{f}_{N'^*\Delta\pi} + \frac{\tilde{g}_{N'^*\Delta\pi}}{\mu^2}\vec{S}^\dagger\cdot\vec{p}_5\vec{S}\cdot\vec{p}_5] \\
&\times[G_1(q^2) + G_2(q^2)p'^0 + G_3(q^2)q^0]\vec{S}^\dagger\cdot\vec{q}
\end{aligned} \tag{71}
$$

Amplitude of N^*(1440):
Vector part :

$$
\begin{aligned}
-iT_8^i &= C\frac{f^*}{\mu}\frac{g_{N^*\Delta\pi}}{\mu}G_\Delta(p_2+p_4)G_{N^*}(p_1+q)\vec{S}\cdot\vec{p}_4\vec{S}^\dagger\cdot\vec{p}_5 \\
&\times\{F_2(q^2)[i\vec{q}\,\frac{q^0}{2m} + (\vec{\sigma}\times\vec{q})(1+\frac{q^0}{2m})] \\
&-F_1(q^2)[i\vec{q}q^0(1+\frac{q^0}{2m}) + q^2\frac{1}{2m}(\vec{\sigma}\times\vec{q})]\}
\end{aligned} \tag{72}
$$

scalar part:

$$
\begin{aligned}
-iT_8^0 &= C\frac{f^*}{\mu}\frac{g_{N^*\Delta\pi}}{\mu}\, G_\Delta(p_2+p_4)G_{N^*}(p_1+q)\vec{S}\cdot\vec{p}_4\vec{S}^\dagger\cdot\vec{p}_5 \\
&\quad\times\{i\frac{\vec{q}^{\,2}}{2m}F_2(q^2)-i\vec{q}^{\,2}(1+\frac{q^0}{2m})F_1(q^2)\}
\end{aligned}
\tag{73}
$$

A5. Amplitudes for the gauge invariant set within Berends formalism.

The explicit amplitudes for the gauge invariant set of the 4 diagrams D1, D2, D4 and D6, in the presence of different form factors are made according to eq. (17) of [25]. We implement them in our formalism by making the following substitutions in the amplitudes shown in the appendix A4. The form factor in the zeroth component of each amplitude is changed as:

T_1^μ:

$$
\frac{\vec{S}^\dagger\cdot\vec{p}_\Delta}{\sqrt{s_\Delta}}F_c \to \frac{\vec{S}^\dagger\cdot\vec{p}_\Delta}{\sqrt{s_\Delta}}F_c-(F_c-1)(\frac{\vec{S}^\dagger\cdot\vec{p}_\Delta}{\sqrt{s_\Delta}}q^0-\vec{S}^\dagger\cdot\vec{q})\frac{q^0}{q^2} \tag{74}
$$

T_2^μ :

$$
F_{\gamma\pi\pi}\{2p_5-q\}^0 \to F_{\gamma\pi\pi}\{2p_5-q\}^0+(F_{\gamma\pi\pi}-1)D_\pi^{-1}\,\frac{q^0}{q^2} \tag{75}
$$

T_4^μ :

$$
F_1^p \to F_1^p+(F_1^p-1)G_N^{-1}\,\frac{q^0}{q^2} \tag{76}
$$

T_6^μ :

$$
F_1^{\Delta^{++}} \to F_1^{\Delta^{++}}+(F_1^{\Delta^{++}}-1)G_\Delta^{-1}\,\frac{q^0}{q^2} \tag{77}
$$

where G_N, G_Δ are the non relativistic propagator of the nucleon and the Δ resonance and D_π the ordinary relativistic pion propagator.

A6. Miscellaneous Formulae.

In order to obtain our amplitudes we have employed some useful relations:

$$
\sum_M S_i|M\rangle\langle M|S_j^\dagger=\frac{2}{3}\delta_{ij}-\frac{i}{3}\epsilon_{ijk}\sigma_k=\delta_{ij}-\frac{1}{3}\sigma_i\sigma_j \tag{78}
$$

$$\sum_{MM'} S_i|M\rangle\langle M|S_{\Delta j}|M'\rangle\langle|M'|S_k^\dagger = \frac{5}{6}i\epsilon_{ijk} - \frac{1}{6}\delta_{ij}\sigma_k + \frac{2}{3}\delta_{ik}\sigma_j - \frac{1}{6}\delta_{jk}\sigma_i \tag{79}$$

From eqs. (78) and (79). we can prove the following relations,which are used in the calculation of the amplitudes:

$$\vec{S}\cdot\vec{p}\vec{S^\dagger}\cdot\vec{q} = \frac{1}{3}[2\vec{p}\cdot\vec{q} - i(\vec{p}\times\vec{q})\cdot\vec{\sigma}] \tag{80}$$

$$\begin{aligned}\vec{S}\cdot\vec{p}(\vec{S_\Delta}\times\vec{k})\cdot\vec{\epsilon}\vec{S^\dagger}\cdot\vec{q} = {} & [\frac{5}{6}i\vec{p}\cdot\vec{\epsilon}\vec{q}\cdot\vec{k} - \frac{5}{6}i\vec{p}\cdot\vec{k}\vec{q}\cdot\vec{\epsilon} - \\ & \frac{1}{6}(\vec{p}\times\vec{k})\cdot\vec{\epsilon}\vec{\sigma}\cdot\vec{q} - \frac{1}{6}\vec{\sigma}\cdot\vec{p}(\vec{q}\times\vec{k})\cdot\vec{\epsilon} + \\ & \frac{2}{3}\vec{p}\cdot\vec{q}(\vec{\sigma}\times\vec{k})\cdot\vec{\epsilon}]\end{aligned} \tag{81}$$

where we have omitted the sum over intermediate states.

References

[1] J.A. Gómez-Tejedor and E. Oset, Nucl. Phys. A571 (1994) 667.

[2] J.A. Gómez-Tejedor and E. Oset, Nucl. Phys. A600 (1996) 413.

[3] A. Braghieri et al., Phys. Lett. B363 (1995) 46.

[4] A. Zabrodin et al., Phys. Rev. C55 (1997) 1617.

[5] F. Härter et al., Phys. Lett. B401 (1997) 229.

[6] L.Y. Murphy and J.M. Laget, DAPHNIA/sphN 95-42, preprint.

[7] J.M. Laget, private communication

[8] K. Ochi, M. Hirata and T. Takaki, Phys. Rev. C56 (1997) 1472.

[9] M. Hirata, K. Ochi and T. Takaki, nucl-th/9711017.

[10] M. Benmerrouche and E. Tomusiak, Phys. Rev. Lett. 73 (1994) 400.

[11] V. Bernard, N. Kaiser, Ulf-G. Meissner and A. Schmidt, Nucl. Phys. A 580. (1994) 475.

[12] V. Bernard, N. Kaiser, and Ulf-G. Meissner, Phys. Rev. Lett.74 (1995) 1036.

[13] M. Benmerrouche and E. Tomusiak, Phys. Rev. Lett. 74 (1995) 1037.

[14] J.A. Gómez-Tejedor, F. Cano and E. Oset, Phys. Lett. B379 (1996) 39.

[15] R. Koniuk and N. Isgur, Phys. Rev. D21 (1980) 1868.

[16] S. Capstick and W. Roberts, Phys. Rev. D49 (1994) 4570.

[17] F. Cano, P. González, B. Desplanques and S. Noguera, Z. Phys. A359 (1997) 819.

[18] J.A. Gómez-Tejedor, M.J. Vicente-Vacas and E. Oset, Nucl. Phys. A588 (1995)

[19] B. Krusche, private communication

[20] S. Kamalov and E. Oset ,Nucl. Phys. A625 (1997) 873.

[21] J.A. Gómez Tejedor, S. Kamalov and E. Oset, Phys. Rev. C54 (1996) 3160.

[22] K. Wacker and G. Drews, Nucl. Phys. B144 (1978) 274,282.

[23] V.Burkert, private communication.

[24] A. Bartl, K. Wittmann, N. Paver, and C. Verzegnassi, Il Nuovo Cimento, 45A(1978) 457

[25] F.A. Berends and R. Gastmans, Phys. Rev. D5 (1972) 204

[26] R.C.E. Devenish, T.S. Eisenschitz and J. G. Korner, Phys. Rev. D11 (1976) 3063.

[27] M. Warns, H. Schröder, W. Pfeil and H. Rollnik, Z. Phys. 45 (1990) 627.

[28] P.J. Mulders, Phys. Reports 185 (1990) 83.

[29] A. Gil and E. Oset, Nucl. Phys. A850 (1994) 513.

[30] E. Amaldi,S. Fubini and G. Furlan, Pion electroproduction, Springer Tracts in Modern Physics, Vol. 83 (Springer, Berlin, 1979)

[31] S. Nozawa and T.S.H. Lee, Nucl. Phys. A513 (1990) 511.

[32] L. Alvarez, S.K. Singh, M.J. Vicente-Vacas, Phys. Rev. C57 (1998) 2693

[33] C. E. Carlson, N. Mukhopadhyay, Phys. Rev. Lett. 13(1998) 2646

[34] C. E. Carlson, Phys. Rev. D34 (1986) 2704

[35] P. Stoler, Phys. Rep. 226 (1993)103

[36] Z. Li, V. Burkert and Z. Li, Phys. Rev. D46 (1992) 70

[37] C. Gerhardt, Z. Phys. C4(1980) 311

[38] V. Burkert, private communication.

[39] A. Gil, J. Nieves, E. Oset, Nucl. Phys. A627 (1997) 553.

[40] H-D. Kiehlmann et al, J. Phys. G:Nucl. Phys. 7(1981) 709-724 and 725-735.

[41] C. Driver et al, Nucl. Phys. B32(1971)45-65.

[42] H.E. Montgomery et al, Nucl. Phys. B51(1973)377-387

[43] A. Bartl et al, Nuovo Cimento 12 (1972) 703

[44] P. Joos et al, Phys. Lett. B62 (1976) 230

[45] Adler et al, Phys. Rev. 169(1967) 1392

[46] P. Carruthers et al, Phys. Lett. B24 (1967) 464

[47] A. Bartl et al, Z. Physik, 269 (1974) 399-406

[48] Aachen-Berlin-Bonn-Hamburg-Heidelberg collaboration, Phys. Rev. 175 (1968) 1669.

A model for $\pi\Delta$ electroproduction on the proton

J.C. Nacher and E. Oset

Departamento de Física Teórica and IFIC

Centro Mixto Universidad de Valencia-CSIC

46100 Burjassot (Valencia)

Spain.

Abstract

We have extended a model for the $\gamma N \to \pi\pi N$ reaction to virtual photons and selected the diagrams which have a Δ in the final state. With this model we have evaluated cross sections for the virtual photon cross section as a function of Q^2 for different energies. The agreement found with the $\gamma_v p \to \Delta^0\pi^+$ and $\gamma_v p \to \Delta^{++}\pi^-$ reactions is good. The sensitivity of the results to $N\Delta$ transition form factors is also studied. The present reaction, selecting a particular final state, is an extra test for models of the $\gamma_v N \to \pi\pi N$ amplitude. The experimental measurement of the different isospin channels for this reaction are encouraged as a means to unravel the dynamics of the two pions photoproduction processes.

1 Introduction

The $\gamma N \to \pi\pi N$ reaction in nuclei has captured some attention recently and has proved to be a source of information on several aspects of resonance formation and decay as well as a test for chiral perturbation theory at low energies. A model for the $\gamma p \to \pi^+\pi^- p$ reaction was developed in [1] containing 67 Feynman diagrams by means of which a good reproduction of the cross section was found up to about $E_\gamma \simeq 1$ GeV.

A more reduced set of diagrams, with 20 terms , was found sufficient to describe the reaction up to $E_\gamma \simeq 800$ MeV [2] where the Mainz experiments are done [3,4,5].

In the same work [2] the model was extended to the other charge channels of $(\gamma, 2\pi)$ and the agreement with the experiment is good except for the channel $\gamma p \to \pi^+\pi^0 n$ where the theoretical cross section underestimates the experiment in about 40 per cent.

Other models have also been recently proposed. The model of ref. [6] contains the dominant terms of [1] and includes some extra resonances in order to make predictions at high energies. A prescription to approximately unitarize the model, of relevance at high energies, is also proposed. Revision of this work is under consideration [7], so more about it should be known in the future.

The model of [8] has fewer diagrams than the one of [1,2] but introduces the $N^*(1520) \to N\rho$ decay mode. By fitting a few parameters to $(\gamma, \pi\pi)$ data the cross sections are reproduced, including the $\gamma p \to \pi^+\pi^0 n$ reaction where the model of [2] fails. The $(\gamma, \pi^0\pi^0)$ channel is somewhat underpredicted. The model of [8] fails to reproduce some invariant mass distributions where the model of [1] shows no problems. A different version of the model of [8] is given in [9], where the parameters of the model are changed in order to reproduce the mass distribution, without spoiling the cross sections. One of the problems in the fit of [9] is that the range parameter of the ρ coupling to baryons is very small, around 200 MeV, which would not be easily accomodated in other areas of the ρ phenomenology, like the isovector πN $s-wave$ scattering amplitude.

On the other hand the model of [2] has no free parameters. All input is obtained from known properties of resonances and their decay, with some unknown sign borrowed from quark models. With all its global success in the different isospin channels, the persistance of the discrepancy in the $\gamma p \to \pi^+\pi^0 n$ channel indicates that further work is needed. The constraints provided by the data in two pion electroproduction should be useful to further test present models and learn more about the dynamics of the two pion production.

The $(\gamma,2\pi)$ reaction has also been used to test chiral perturbation theory. The threshold region is investigated in [10,11] with some discrepancies in the results which are commented in [12,13]. The one loop corrections are shown to be relevant in the $\gamma p \to \pi^0\pi^0 p$ reaction close to threshold [11]. In addition the $N^*(1440)$ excitation is shown to be very important at threshold in [2].

Another interesting information obtained from the $\gamma p \to \pi^+\pi^- p$ reaction is

information about the $N^*(1520)$ decay into $\Delta\pi$. Indeed, the photoexcitation of the $N^*(1520)$ followed by the decay into $\Delta\pi$ is a mechanism which interferes with the dominant term, the $\gamma N\Delta\pi$ Kroll-Ruderman term, and offers information on the q dependence and the sign of the s and $d-wave$ amplitudes of $N^*(1520) \to \Delta N$ decay. This information is a good test of quark models [14] which is passed by the "relativised" constituent quark models [15,16,17]. In the $\gamma p \to \pi^0\pi^0 p$ reaction the $\gamma N \to N^*(1520) \to \Delta\pi$ is shown to be an important mechanism by itself (there is no Δ Kroll-Ruderman term here), and it is perfectly visible in the experimental invariant mass distribution [5].

The (γ,2π) reaction has also relevance in nuclear physics. Inclusive cross section for the (γ,$\pi^+\pi^-$) have been calculated in [18] and the inclusive (γ,$\pi^0\pi^0$) reaction is measured in [19]. Calculations for (γ,$\pi^+\pi^-$) and the (γ,$\pi^0\pi^0$) coherent two pion production in nuclei have been performed in [20] and the cross sections are found to be very different in two different charge channels, with patterns in the energy and angular distributions linked to isospin conservation. Similarly, exchange currents for the (γ,π^+) reaction are constructed from (γ,$\pi\pi$) when a pion is produced off-shell and absorbed by a second nucleon. These exchange currents give an important contribution to the (γ,π^+) cross section at large momentum transfer [21].

The discussions above have served to show the relevance of the (γ,2π) reaction and its implications in different processes. The extension of this kind of work to virtual photons should complement the knowledge obtained through the (γ,2π) and the related reactions. The coupling of the photons to the resonances depends on q^2 and the dependence can be different for different resonances. Hence, the interference of different mechanisms pointed above will depend on q^2 and with a sufficiently large range of q^2, one can pin down the mechanism of (γ,2π) with real or virtual photons with more precision than just with real photons, which would help settle the differences between present theoretical models.

However, there are already interesting two pion electroproduction experiments selecting Δ in the final state. The reactions are, $ep \to e'\pi^+\Delta^{++}$ and $ep \to e'\pi^+\Delta^0$ [22]. It is thus quite interesting to extend present models of $(\gamma, 2\pi)$ to the realm of virtual phtons and compare with existing data. In the present paper we do so, extending the model of ref.[2] to deal with the electroproduction process. This model is flexible enough and one can select the diagrams which contain $\Delta\pi$ in the final state in order to compare directly with the measured cross sections.

The extension of the model requires three new ingredients: the introduction of the zeroth component of the photon coupling to resonances (calculations where done in [2] in the Coulomb gauge, ϵ^0, where the zeroth component is not needed), the implementation of the q^2 dependence of the amplitudes, which will be discussed in forthcoming sessions, and the addition of the explicit terms linked to the $S_{1/2}$ helicity amplitudes which vanish for real photons.

Experiments on (γ_v,2π) are presently being done in the Thomas Jefferson Laboratory [23], both for $N\Delta$ and $N\pi\pi$ production.

The model presented here can serve to extract relevant information from coming data, which will improve appreciably the precission of present experiments.

There has been earlier work on the particular problem which we are discussing here. In [24] an approach for $\Delta\pi$ electroproduction close to threshold was done with special emphasis in determining the axial transition form factors. The approach uses the current algebra formalism and some of the input needed is obtained from the same electroproduction data. The delta is treated as an elementary particle but the cross sections are folded with a Breit Wigner distribution in order to take into account approximately the effects of the finite width of the Δ. The effects of the D_{13} resonance are also discussed and introduced in an approximate way. The novelties here with respect to this work would be the use of a different formalism, since we are relying on the Feynman diagrammatic approach. On the other hand all information needed here, some of which was not available at the time of ref.[24], is already known such that clear predictions can be made. There is another important difference with respect to [24] which is that the Δ is not considered as a final state but decays explicitly into πN in the Feynman diagrams considered. This means that the Δ is treated as a propagator and the sum over polarizations is done in the amplitudes not in the cross sections as in [24]. This allows one to keep track of angular correlations between the two pions which are lost if the Δ is considered as a final state. It also allows to take into account the delta width in a natural way since it just comes as the imaginary part of the inverse of the Δ propagator. It also allows one to keep track of interference of different pieces, in particular those between the Δ Kroll Ruderman term and the excitation of the $N^*(1520)$ resonance followed by $\Delta\pi$ decay, which is one of the important findings in the present reaction.

Our model bears more similarity to the work of [25] where also a diagrammatic approach is followed. They introduce the minimal set of terms which are gauge invariant as a block, including the important Δ Kroll Ruderman term. In our model we also include the four terms of [25] but we have in addition four more terms, in particular the excitation of the $N^*(1520)$ resonance followed by $\Delta\pi$ decay, which has a strong interference with the Δ Kroll Ruderman term. In [25] a formalism is used which respects Ward identities and leads to a gauge invariant amplitude in the presence of different electromagnetic form factors for the different terms of the model appearing for virtual photons. We have also followed this formalism in our approach.

For the construction of the currents for resonance excitation we follow closely the work of [26] and take the convention of [27] for the definition of the helicity amplitudes. Altogether the formalism in the present paper diverts somewhat from the one used for real photons in [1,2] where many simplifications could be done, but in the case of real photons we regain the results of [1,2], although the use of new conventions forces the change of some sign. In order to avoid confusion the Lagrangians used and new conventions are now written in detail in a section.

2 Model for $eN \to e'\Delta\pi$.

We will evaluate cross sections of virtual photons integrated over all the variables of the pions and the outgoing nucleon. In this case the formalism is identical to the one of inclusive $eN \to e'X$ scattering [28,29] or pion electroproduction after integrating over the pion variables [30,31]. The (e, e') cross section is given by

$$\begin{aligned} \frac{d\sigma}{d\Omega' dE'} &= \frac{\alpha^2}{q^4}\frac{k'}{k}\frac{-q^2}{1-\epsilon}\frac{1}{2\pi e^2}[(W^{xx}+W^{yy})+ \\ &\quad 2\epsilon(\frac{-q^2}{\vec{q}^2})W^{00}] \end{aligned} \tag{1}$$

where $\alpha = e^2/4\pi$ is the fine structure constant, e the electron charge, q^μ the momentum of the virtual photon and k, k' the momenta of the initial and the final electron and ϵ the polarization parameter of the photon, which is given by

$$\epsilon = [1 - \frac{2\vec{q}^2}{q^2} tg^2 \frac{\theta_e}{2}]^{-1} \tag{2}$$

with θ_e the angle of the scattered electron. All variables are given in the lab frame and the z direction is taken along the direction of the virtual photon, $\vec{q}$. Furthermore, the hadronic tensor is given here by

$$\begin{aligned} W^{\mu\nu} &= \int \frac{d^3p_2}{(2\pi)^3}\frac{M}{E_1}\frac{M}{E_2}\int \frac{d^3p_4}{(2\pi)^3}\frac{1}{2w_4}\int \frac{d^3p_5}{(2\pi)^3}\frac{1}{2w_5} \\ &\quad \overline{\sum}\sum T^\mu T^{\nu *}(2\pi)^4\delta(q+p_1-p_2-p_4-p_5) \end{aligned} \tag{3}$$

where p_1, p_2, p_4, p_5 are the momenta of the initial, final nucleon, and the two pions and T^μ is the matrix element of the $\gamma_v N_1 \to N_2\pi_4\pi_5$ process. Note that the phase space accounts for the decay of the Δ into $N\pi$ explicitly, hence the finite width of the Δ is automatically taken into account. The terms contributing to T^μ are given below.

The expression of eq.(1) can be conveniently rewritten as [30]

$$\frac{d\sigma}{d\Omega' dE'} = \Gamma(\sigma^T_{\gamma_v} + \epsilon\sigma^L_{\gamma_v}) = \Gamma\sigma_{\gamma_v} \tag{4}$$

where $\sigma^T_{\gamma_v}$, $\sigma^L_{\gamma_v}$ are the transverse,longitudinal cross sections of the virtual photons and Γ is given by

$$\Gamma = \frac{\alpha}{2\pi^2}\frac{1}{-q^2}\frac{k'}{k}\frac{1}{1-\epsilon}K_\gamma \tag{5}$$

$$K_\gamma = \frac{s-M^2}{2M} \quad ; s = (q^0+M)^2 - \vec{q}^2 \tag{6}$$

The corresponding cross sections $\sigma^T_{\gamma_v}$ and $\sigma^L_{\gamma_v}$ are easily induced from eqs. (1) and (4). The term with the combination $W^{xx} + W^{yy}$ in eq. (1) gives rise

to the transverse cross section while the term proportional to W^{00} gives rise to the longitudinal one.

In the limit of the real photons, when $q^2 \simeq 0$, K_γ is the lab momentum of the photon, and only the transverse cross section contributes, in which case $\sigma^T_{\gamma_v} = \sigma_\gamma$, the cross section of real photons.

For the model of the $\gamma_v N \to \Delta\pi$ reaction we take the same diagrammatic approach as in ref.[2] and select the diagrams which have a Δ in the final state. The diagrams which contribute to the process are depicted in fig.1. The contribution of each one of the diagrams is readily evaluated from the Lagrangians written in appendix A1. The Feynman rules for the diagrams are collected in appendix A2. The coefficients, coupling constants and the form factors are collected in appendix A3. Finally, the amplitudes for each one of the terms are written in appendix A4 for each charge state.

Out of the 20 terms in [2] for the general $(\gamma, 2\pi)$ reaction only 8 terms contain a Δ and a pion in the final state which are the terms collected in fig.1.

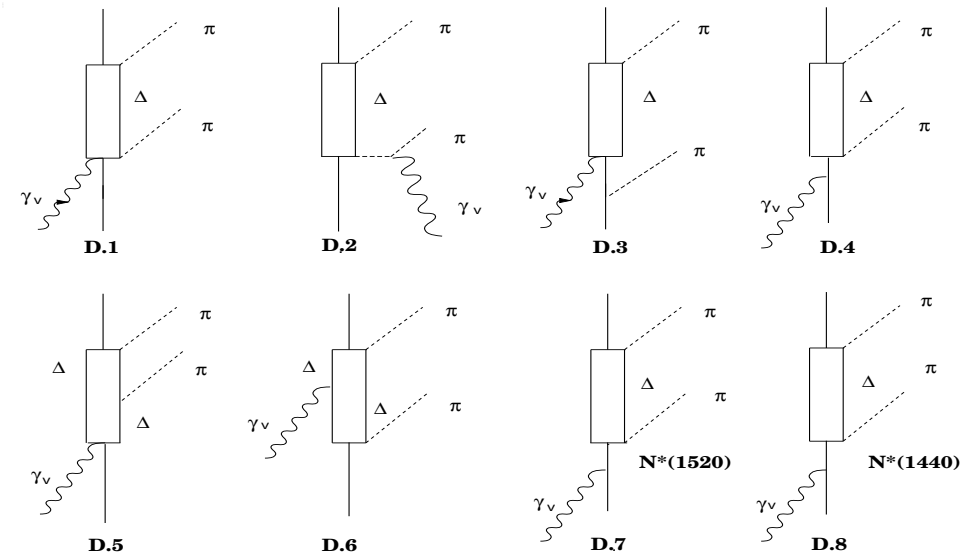

Fig.1

Figure 1: Feynman diagrams used in the model for $\gamma_v p \to \pi\Delta$

3 Electromagnetic transitions for Roper and N*(1520) resonances

We follow the paper from Devenish et al. [26] in our approach to these transitions. As we are working with virtual photons we need to care about these couplings and hence include terms which vanish for real photons. For the diagram D.8, which involves the Roper excitation as depicted in the fig. 1, we

can write the corresponding electromagnetic current as :

$$J^{\mu}_{e.m.} = \bar{u}_{N^*}(p')[\frac{\bar{F}_2(q^2) i\sigma^{\mu\nu} q_\nu}{m+m^*} + \bar{F}_3(q^2)(q^\mu - \frac{q^2}{m^*-m}\gamma^\mu)]u_N(p) \quad (7)$$

where $\bar{F}_{2,3}(q^2)$ are the electromagnetic form factors for the $N - N^*$ transition (which already include the proton charge), $q^\mu = (q^0, \vec{q})$ is the momentum of the virtual photon and the m, m^* the masses of the nucleon and the $N^*(1440)$ respectively. We can rewrite these form factors in terms of F_1, F_2, defined as: $F_1 = \frac{\bar{F}_3}{m^*-m}$ and $F_2 = \frac{\bar{F}_2}{m+m^*}$. The current of eq. (7) coincides with the one in [26] substituting there: $G_1 = -F_1$ and $G_2 = -\frac{2F_2}{m^*-m}$. We write our vertex functions as $V^\mu \epsilon_\mu = -iJ^\mu \epsilon_\mu$. By keeping terms up to (q/m) in a non relativistic reduction of the matrix elements of the Dirac gamma matrices we find:

$$V^{\mu}_{\gamma N N^*} = \left\{ \begin{array}{c} i\frac{\vec{q}^2}{2m} F_2(q^2) - i\vec{q}^2(1+\frac{q^0}{2m})F_1(q^2) \\ F_2(q^2)[i\vec{q}\,\frac{q^0}{2m} + (\vec{\sigma}\times\vec{q})(1+\frac{q^0}{2m})] - F_1(q^2)[i\vec{q}q^0(1+\frac{q^0}{2m}) + q^2\frac{1}{2m}(\vec{\sigma}\times\vec{q})] \end{array} \right\} (8)$$

Next we construct the helicity amplitudes for our transition. There are many works where the helicity amplitudes are calculated [27, 32, 33, 34, 35]. In what follows we adjust to the formalism of ref. [27]. Then $A_{1/2}$ and $S_{1/2}$ can be written as:

$$A^{N^*}_{1/2} = \sqrt{\frac{2\pi\alpha}{q_R}}\frac{1}{e}\langle N^*, J_z = 1/2|\epsilon^{(+)}_\mu \cdot J^\mu|N, S_z = -1/2\rangle \quad (9)$$

$$S^{N^*}_{1/2} = \sqrt{\frac{2\pi\alpha}{q_R}}\frac{|\vec{q}|}{\sqrt{Q^2}}\frac{1}{e}\langle N^*, J_z = 1/2|\epsilon^{(0)}_\mu \cdot J^\mu|N, S_z = 1/2\rangle \quad (10)$$

where q_R is the energy of an equivalent real photon, $(W^2 - m^2)/(2W)$ and W is the photon-proton center of mass energy.

The tranverse polarization vectors are:

$$\epsilon^{(\pm)}_\mu = \frac{(0, \mp 1, -i, 0)}{\sqrt{2}} \quad (11)$$

and $\epsilon^0_\mu = \frac{1}{\sqrt{Q^2}}(q, 0, 0, q^0)$ normalized to unity, satisfying $\epsilon^0_\mu \cdot q^\mu = g^{\mu\nu}\epsilon^0_\mu \cdot \epsilon^{(\pm)}_\nu = 0$ with $\vec{q}$ in z direction and $Q^2 = -q^2$.

Using our electromagnetic current the helicity amplitudes are given by:

$$A^{N^*}_{1/2} = \sqrt{\frac{2\pi\alpha}{q_R}}\frac{1}{e}[F_2(q^2)\sqrt{2}q(1+\frac{q^0}{2m}) + F_1(q^2)Q^2\sqrt{2}\frac{q}{2m}] \quad (12)$$

and

$$S^{N^*}_{1/2} = \sqrt{\frac{2\pi\alpha}{q_R}}\frac{\vec{q}^2}{e}[-F_2(q^2)\frac{1}{2m} + F_1(q^2)(1+\frac{q^0}{2m})] \quad (13)$$

Inverting these equations we can get the electromagnetic form factors in terms of the helicity amplitudes. The experimental helicity amplitudes $A^p_{1/2}$ and $S^p_{1/2}$ which we use are taken from [36] which uses data from [37].

In the case of the $N^*(1520)$ resonance we can take the same steps as above. Following [26] we write the relativistic current as:

$$J^\mu_{e.m.} = G_1(q^2)J^\mu_1 + G_2(q^2)J^\mu_2 + G_3(q^2)J^\mu_3 \tag{14}$$

with

$$J^\mu_1 = \bar{u}_\beta(q^\beta\gamma^\mu - \not{q}g^{\beta\mu})u \tag{15}$$

$$J^\mu_2 = \bar{u}_\beta(q^\beta p'^\mu - p'\cdot q g^{\beta\mu})u \tag{16}$$

$$J^\mu_3 = \bar{u}_\beta(q^\beta q^\mu - q^2 g^{\beta\mu})u \tag{17}$$

and G_1,G_2,G_3 are the electromagnetic form factors for this vertex and p' is the momenta of the resonance.

Taking a non relativistic reduction as done before and using u_μ Rarita-Schwinger spinors in the c.m. of the resonance, the vertex takes an expression given by:

Scalar part:

$$V^0_{\gamma NN'^*} = i(G_1 + G_2 p'^0 + G_3 q^0)\vec{S}^\dagger\cdot\vec{q} \tag{18}$$

and the vector part:

$$\begin{aligned} V^i_{\gamma NN'^*} = -i[&(\frac{G_1}{2m} - G_3)(\vec{S}^\dagger\cdot\vec{q})\,\vec{q} - \\ &iG_1\frac{\vec{S}^\dagger\cdot\vec{q}}{2m}(\vec{\sigma}\times\vec{q}) - \vec{S}^\dagger\{G_1(q^0 + \frac{\vec{q}^{\,2}}{2m}) + G_2 p'^0 q^0 + G_3 q^2\}] \end{aligned} \tag{19}$$

Using again eqs.(9) and (10) we calculate the $A_{1/2}$ and $S_{1/2}$ helicity amplitudes for the $N^*(1520)$. In addition, in this case we also have the $A_{3/2}$ helicity amplitude which is given in [27] by:

$$A^{N^*}_{3/2} = \sqrt{\frac{2\pi\alpha}{q_R}}\frac{1}{e}\langle N^*, J_z = 3/2|\epsilon^{(+)}_\mu\cdot J^\mu|N, S_z = 1/2\rangle \tag{20}$$

The expressions for the helicity amplitudes obtained using the current in eqs.(14-17) are:

$$A^{N'^*}_{3/2} = \sqrt{\frac{2\pi\alpha}{q_R}}\frac{1}{e}[G_1(q^0 + \frac{\vec{q}^{\,2}}{2m}) + G_2 q^0 p'^0 + G_3 q^2] \tag{21}$$

$$A^{N'^*}_{1/2} = \sqrt{\frac{2\pi\alpha}{q_R}}\frac{1}{e}\frac{1}{\sqrt{3}}[G_1(q^0 - \frac{\vec{q}^{\,2}}{2m}) + G_2 q^0 p'^0 + G_3 q^2] \tag{22}$$

$$S_{1/2}^{N'*} = -\sqrt{\frac{2\pi\alpha}{q_R}}\frac{1}{e}\sqrt{\frac{2}{3}}q[G_1 + G_2 p'^0 + G_3 q^0] \tag{23}$$

From these three equations we can get the G_1, G_2, G_3 form factors in terms of the helicity amplitudes. The data for $S_{1/2}$ are taken from [27] and for $A_{1/2}$ and $A_{3/2}$ from [27, 38] [1].

The other important vertex in our model corresponds to the $\Delta - N$ electromagnetic transition. As discussed in [32, 33], the most important transition is the magnetic dipole (M_{1+}) transition while the electric quadrupole (E_{1+}) and scalar quadrupole (S_{1+}) transitions are small at momentum transfers between the photon point to Q^2=1.3 GeV^2. The values given in [26] for the ratio E_{1+}/M_{1+} (S_{1+}/M_{1+}) are -0.02 to 0.02 (-0.025 to -0.06) for Q^2=0 to 1.3 GeV^2 respectively. We take the $\gamma N\Delta$ transition current from [39] where the same non relativistic expansion done here, keeping terms of order $O(p/m)$ for the Dirac matrix elements, is done. A good reproduction of the data for electroproduction of one pion was obtained there in a wide range of energies around the Δ resonance and different Q^2. The vertex for this electroproduction transition is given by eq. (40) in appendix A2 and the form factor used is given by eq. (61) in appendix A3.

4 Gauge invariance and form factors

Gauge invariance is one of the important elements in a model involving photons and implies that

$$T^\mu q_\mu = 0 \tag{24}$$

The explicit expressions for T^μ, keeping the four components, as given in appendix A4, allow one to check explicitly the gauge invariance. The block of diagrams D1, D2, D4 and D6 form together a gauge invariant set. The rest of the diagrams in which the photon directly excites a resonance from a nucleon are gauge invariant by themselves. However, some caution must be observed when imposing eq. (24). Indeed, in diagram D2 the intermediate pion is off-shell and induces a strong $\pi N\Delta$ transition form factor, $F_\pi(p^2)$, for which we take a usual monopole form factor (see eq.(53) appendix A3). The constraints of eq.(24) forces this form factor to appear in the other terms of the block of diagrams which are gauge invariant. However, as discussed in the study of the $eN \to e'N\pi$ reaction in [39], and as can be easily seen by inspection of the diagrams and the amplitudes, the constraint of eq. (24) still requires the equality of four electromagnetic form factors,

$$F_1^p(q^2) = F_1^\Delta(q^2) = F_{\gamma\pi\pi} = F_c(q^2) \tag{25}$$

[1] We note that the formalism followed here for the vertices of the $N^*(1520)$ is different from that of [2], but the same results are obtained for real photons.

The form factors of eq. (25), if the strict Feynmann rules of the appendix A4 are followed, are respectively the γNN, $\gamma\Delta\Delta$, $\gamma\pi\pi$ and $\gamma\Delta N\pi$ ones. These form factors are usually parametrized in different forms, as seen in appendix A3, except for $F_1^p(q^2)$ and $F_1^\Delta(q^2)$ which are taken equal, as it would come from ordinary quark models.

Although the model is gauge invariant with the prescription of eq. (25) there is the inconvenience that the results depend upon which one of the three form factors we take for all of them.

In the next section we discuss the uncertainties which come from this arbitrary choice of form factor. We should note however, that the dominant term, by large, is the Δ Kroll Ruderman and pion pole terms. This is also so in the test of gauge invariance where the two terms involving the $F_1^p(q^2)$ form factor in diagrams D4, D6 give only recoil contributions of the order of $\mathrm{O}(p_\pi/\mathrm{m})$ in eq. (24). This justifies the use of $F_c(q^2)$ or $F_{\gamma\pi\pi}(q^2)$ for all the form factors.

There is, however, another way to respect gauge invariance, while at the same time using different form factors which is proposed in [25] and to which we refer in what follows as Berends et al. approach. In the next section we will show the results from both approaches and will discuss them.

There are many papers in the literature following the Berends et al. approach in order to explain the experimental results with this gauge invariant set of diagrams [40, 41, 42, 43].

Another of the common approaches to this problem in the past has been the use of current algebra [44, 45, 46]. In this case, close to threshold of $\Delta\pi$ production, the axial vector current $\langle\Delta|A_\mu|N\rangle$ is the dominant term. In the soft pion limit this axial vector current is shown to be equivalent [45] to the one of the nucleon. The $\pi\Delta$ electroproduction data are hence used in those works to determine the nucleon axial form factor.

Our model is more general since one obtains explicit p_π^μ dependence, for instance from the pion pole term (diagram D.2 fig. 1). The dominance of the $\Delta N\pi\gamma$ Kroll Ruderman at threshold (independent of p_π^μ) offers however some support to the assumptions made in those works, as quoted in [30]. The diagrammatic approach relies however on the explicit use of the four form factors of eq. (25). We shall see in the next section the influence of the different terms close to threshold.

In [47], following the diagrammatic approach with the minimal set of gauge invariant terms, fits to the data are carried fixing $F_{\gamma\pi\pi}$ from ρ vector meson dominance and setting the other three form factors equal in order to determine this latter common form factor. A qualitative agreement with the $F_1^p(q^2)$ form factor obtained from others sources is found.

With the gauge invariant prescription of [25] using different form factors, different fits to the data are carried fixing some of the form factors and determining others. We shall follow this latter approach , but with our enlarged set of Feynman diagrams including the explicit decay of the Δ into πN, which allows one to keep track of correlations between the pions if wished. We will show the sensitivity of the results to different form factors and the weight of

the different terms as a function of energy and Q^2.

The explicit formulas of the gauge invariant set in the presence of the different form factors are taken from eq. (17) of ref. [25] and, after the non relativistic reduction is done, the expressions used here are shown in appendix A5.

5 Results and discussion

We have tested our results with the experimental data of refs. [22,30]. We show the cross section of $\gamma_v p \to \Delta^{++}\pi^-$ and $\gamma_v p \to \Delta^0\pi^+$ ($\Delta^0 \to \pi^- p$), as a function of W, the virtual photon-proton ($\gamma_v p$) center of mass energy, and for different values of Q^2. We have

$$W^2 = -Q^2 + M^2 + 2M\nu\,; \nu = E - E' \tag{26}$$

with

$$Q^2 = -q^2 = 4EE' sin^2(\frac{\theta_e}{2}) \tag{27}$$

We compare in fig. 2 the results for delta photoproduction (real photons) with the experimental data [48] and we see that the agreement found is quite satisfactory.

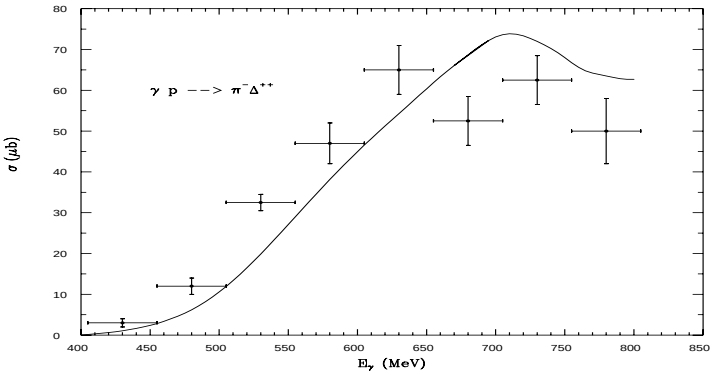

Figure 2: Cross section for the $\gamma p \to \Delta^{++}\pi^-$ reaction. Experimental data from [48].

In order to compare our results with experiment for virtual photons we calculate first the cross sections at $Q^2 = 0.6\ GeV^2$.

Figure 3 contains three different calculations. Two of them correspond to using all form factors equal (which we set to $F_{\gamma\pi\pi}$) with two different values of λ_π^2, 0.5 GeV^2 and 0.6 GeV^2. We see that the cross section increases by about 10 % when going from λ_π^2=0.5 GeV^2 and λ_π^2=0.6 GeV^2. We also show the results taking F_1^p, F_1^Δ with their values given in appendix A3 and setting $F_c = F_{\gamma\pi\pi}$ with λ_π^2=0.6 GeV^2. This latter calculation is not gauge invariant.

However we see that the deviation with respect to the gauge invariant one assuming all form factors equal is very small. This reflects the fact that the relevant terms in the model are those involving $F_{\gamma\pi\pi}$ and F_c, the pion pole and Δ Kroll Ruderman terms.

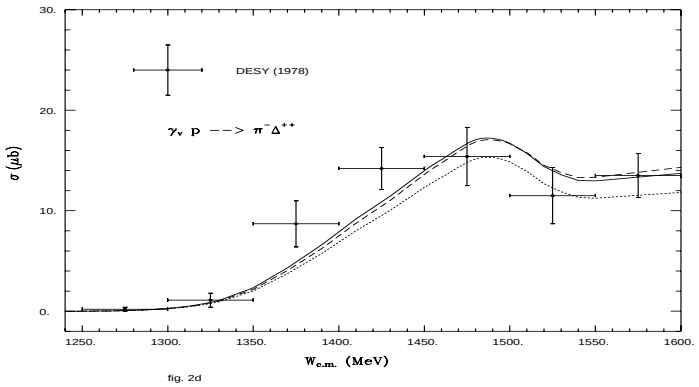

Figure 3: Cross section for $\gamma_v p \to \pi^- \Delta^{++}$ as a function of the $\gamma_v p$ center of mass energy. The curves correspond to $Q^2 = 0.6\ GeV^2$. Dashed line: F_1^p, F_1^Δ, from appendix A3 and F_c=$F_{\gamma\pi\pi}$ with $\lambda_\pi^2 = 0.6\ GeV^2$. Continuous line: $F_1^p = F_1^\Delta = F_c = F_{\gamma\pi\pi}$ with $\lambda_\pi^2 = 0.6\ GeV^2$. Dotted line: same as continuous line with $\lambda_\pi^2 = 0.5\ GeV^2$

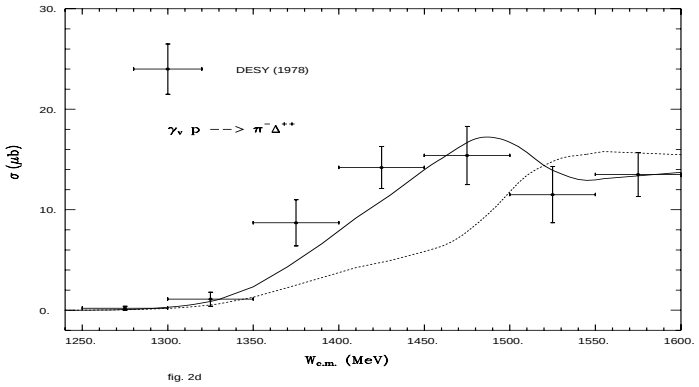

Figure 4: Continuous line: Cross section for $\gamma_v p \to \pi^- \Delta^{++}$ at Q^2= 0.6 GeV^2 using $F_1^p = F_1^\Delta = F_{\gamma\pi\pi} = F_c$ with λ_π^2=0.6 GeV^2 and $\tilde{f}_{N^{*\prime}\Delta\pi} = -0.911$, $\tilde{g}_{N^{*\prime}\Delta\pi}$=0.552. Dotted line: same as continuous line but with $\tilde{f}_{N^{*\prime}\Delta\pi}$=0.911 and $\tilde{g}_{N^{*\prime}\Delta\pi} = -0.552$. See appendices A1 and A2 for the vertices and coupling constants used.

In refs. [2,14], two solutions for the coupling of the $N^*(1520)$ to the Δ in s and $d-waves$, differring only in a global sign, were found from the respective decay widths. Only a sign was compatible with the experimental $(\gamma, \pi\pi)$ data, because of the strong interference between the $\gamma N \to N^*(1520) \to \Delta\pi$ term and the Kroll Rudermam one. Here, in the new formalism the amplitude of the $\gamma N \to N^*(1520)$ transition changes sign and consequently the signs of the former $N^*(1520) \to \Delta\pi$ couplings must be changed. In fig. 4 we show the results of $\gamma_v p \to \pi^- \Delta^{++}$ at Q^2=0.6 GeV^2 using the two different signs for these

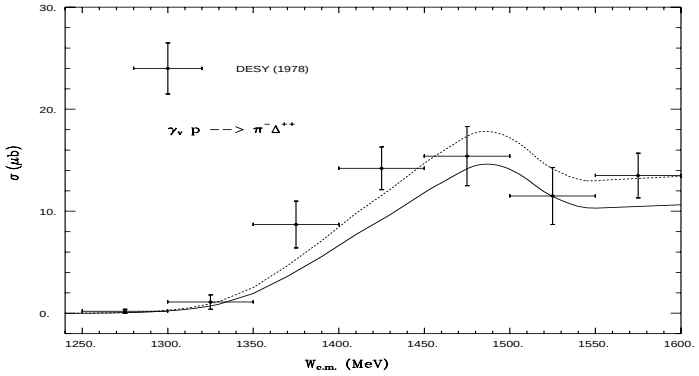

Figure 5: Cross sections from $\gamma_v p \to \Delta^{++}\pi^-$ with Berends formalism included. Continuous line: $F_1^p, F_1^\Delta, F_{\gamma\pi\pi} = F_c$ with $\lambda_\pi^2 = 0.5\ GeV^2$. Dotted line: same as continuous line with the parameter for $F_{\gamma\pi\pi}$ 0.5 GeV^2 and for F_c is 0.8 GeV^2.

couplings. We can see that the data favour clearly one of the signs. This was also observed in the $\gamma p \to \pi^+\pi^- p$ reaction in [14]. Fig. 4 shows the magnitude of the interference between those terms. Neglecting the $\gamma p \to N^*(1520) \to \Delta\pi$ process leads to results in between the two curves shown in the figure where one does not see any peak. The peak shown by the data around W=1480 MeV is hence not reminiscent of a Δ but a peak coming from the constructive interference of the terms mentioned above.

Now we evaluate the cross section using Berends gauge invariant approach with different form factors [25] using the formulae of appendix A5 for the set of the four gauge invariant terms. We show the results in fig. 5. The continuous line in the figure is obtained with this prescription using the form factors of appendix A3 for the F_1^p, F_1^Δ but setting $F_c = F_{\gamma\pi\pi}$ with $\lambda_\pi^2 = 0.5\ GeV^2$.

We can see that these results are remarkably similar to those of the dotted line in fig. 3 where F_c and $F_{\gamma\pi\pi}$ had the same values as here but F_1^p, F_1^Δ were set equal to $F_{\gamma\pi\pi}$ in order to preserve gauge invariance.

Once again we can see that the terms involving F_1^p and F_1^Δ are relatively unimportant, or in any case that setting these form factors equal to $F_{\gamma\pi\pi}$ provide a gauge invariant result very close to the one obtained with the more general Berends prescription of [25].

The dotted line in fig. 5 corresponds to the same parametrization for F_c as for $F_{\gamma\pi\pi}$ but parameter λ_c^2= 0.8 GeV^2. This shows the sensitivity of the results to F_c which appears in the dominant Kroll-Ruderman term.

Given the dominance of the Kroll Ruderman term close to threshold production of $\Delta\pi$ in our model and the dominance of the terms involving the axial form factor in the current algebra approaches, we now show in fig. 6 the results taking for F_c the parametrization of the axial vector form factor (see appendix A3), varying the value of M_A. The Berends formalism with different form factors is used, and F_1^p, F_1^Δ, $F_{\gamma\pi\pi}$ are taken as in appendix A3. We can see that the experimental data favour values of $M_A \simeq$ 1.16-1.23 GeV very similar to the values determined in [30] (1.16$\pm$ 0.03) GeV or [44] (1.18$\pm$ 0.07)

GeV.

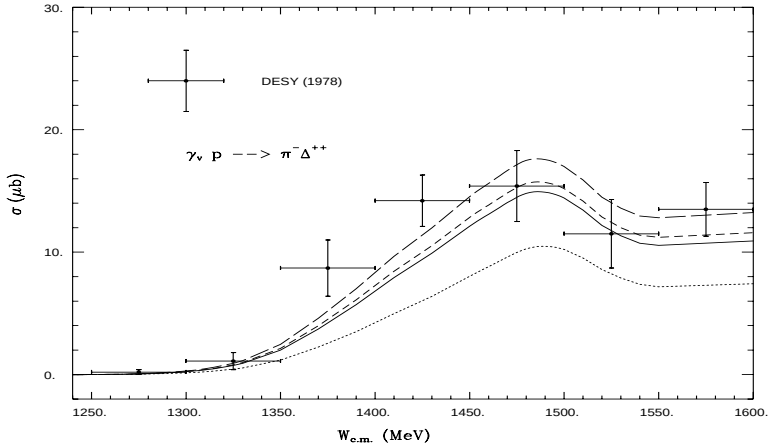

Figure 6: Cross sections for $\gamma_v p \to \pi^- \Delta^{++}$ within Berends formalism. We use different form factors for F_1^p, F_1^Δ, $F_{\gamma\pi\pi}$ from appendix A3. We take for the axial form factor, F_A, form the contact term. The parameter M_A is changed from up to down :1.32, 1.23, 1.16, 0.89 in GeV.

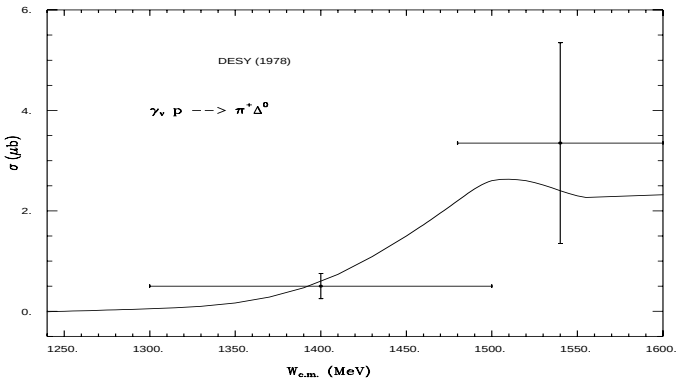

Figure 7: Cross section for $\gamma_v p \to \pi^+ \Delta^0$ within Berends formalism. We use $F_1^p, F_1^\Delta, F_{\gamma\pi\pi}$ from appendix A3 and F_A with M_A=1.16 GeV.

In fig. 7 we show the cross section for $\gamma_v p \to \Delta^0 \pi^+$ with Berends scheme and with a value of the axial form factor parameter of $M_A = 1.16$ GeV. We find a good agreement with the scarce experimental data but more data would be required to further check this channel.

In all these sets of figures for Δ^{++} electroproduction we find a good agreement with the experimental results around the peak region 1460 MeV$\leq$ W $\leq$ 1600 MeV in c.m. energy at Q^2=0.6 GeV^2. As commented above, this peak comes from the interference between the Δ Kroll Ruderman and the $N^*(1520)$ excitation terms, which was also found for real photons in [1,2,14]. A priori this interference pattern could change for virtual photons since these two terms are affected by different form factors, $F_c(q^2)$ for the contact term and the form

factors $G_1(q^2), G_2(q^2), G_3(q^2)$ that appear for the $\gamma N \to N^*(1520)$ transition. In practice we see that the interference survives in the case of virtual photons.

The $N^*(1520)$ excitation has a longitudinal coupling and so has the Δ. The inclusion of this longitudinal contribution could also blur the interference found with these two terms for real photons. However, the results shown for virtual photons show that the interference remains also in this latter case. We have checked that if we go up to higher Q^2 the interference still exists but the shape becomes flatter.

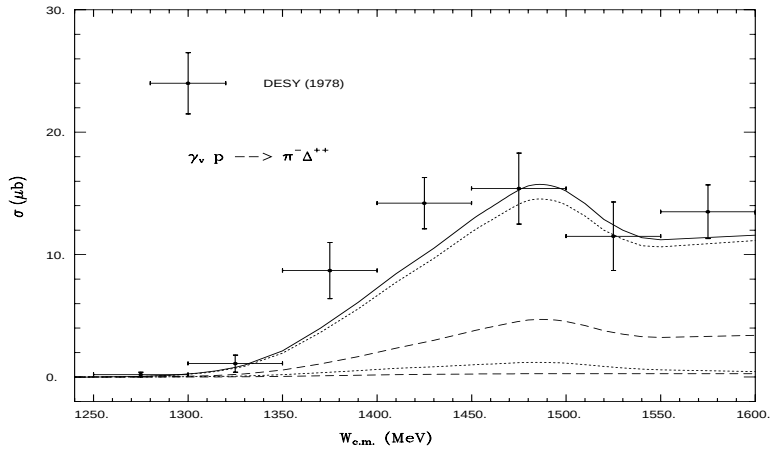

Figure 8: Continuous line: cross section for $\gamma_v p \to \Delta^{++}\pi^-$ within Berends formalism and with the parameter M_A=1.23 GeV at Q^2=0.6 GeV^2. Dotted lines: From up to down we show the tranverse σ_T and longitudinal $\epsilon\sigma_L$ cross section at Q^2=0.6 GeV^2 respectively. Short-dashed lines: From up to down the same as in dotted line for Q^2=1.2 GeV^2.

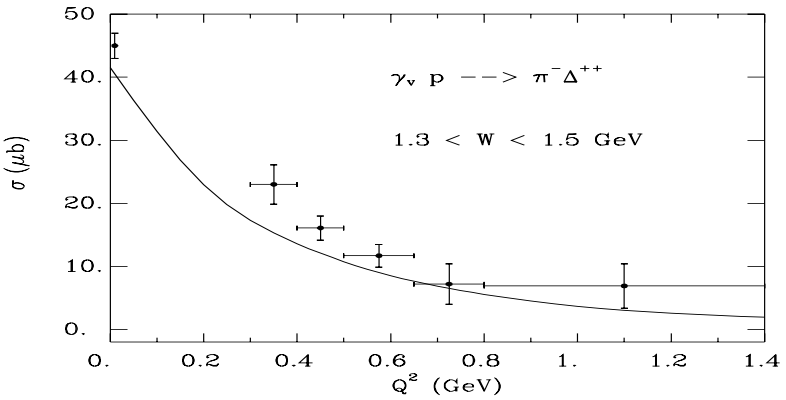

Figure 9: Cross section $\gamma_v p \to \Delta^{++}\pi^-$ as a function of the Q^2.

It is interesting to show separate contributions for the longitudinal and transverse cross sections which are likely to be also measured at TJNAF. We

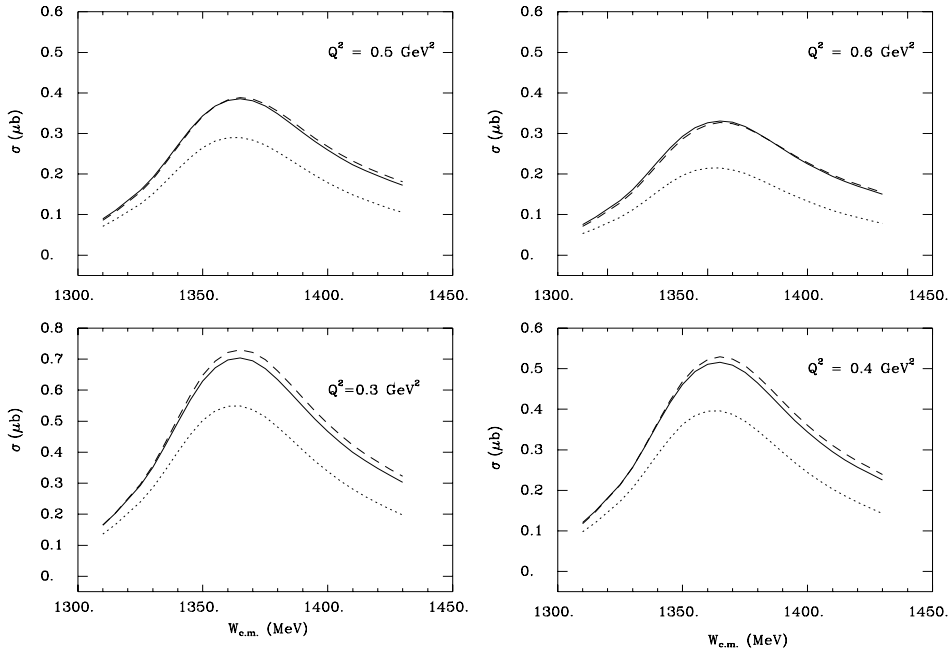

Figure 10: Continuous line: Total cross section from $\gamma_v \to \pi^- \Delta^{++}$ within Berens formalism restricting $m_\pi \leq \omega_{\pi^-} \leq m_\pi + 10$ MeV. We use F_1^p, F_1^Δ from appendix A3 and $F_{\gamma\pi\pi}$ with λ_π^2= 0.5 GeV^2. Dotted lined: Contribution of Δ Kroll Ruderman term using F_A with M_A=1.16 GeV. Short-dashed line: Contribution of Δ Kroll Ruderman term plus the interference with the $N^*(1520)$ term.

.

find in fig. 8 that the shape of the curves for the transverse contribution is the same as for real photons and for the sum of the longitudinal and transverse cross sections for the virtual ones. We observe that the longitudinal contribution gives only a small background. This pattern appears for any intermediate values of Q^2 between those shown in the figure.

In fig. 9 we show a cross section as a function of the momentum transfer Q^2 and we compare with the experimental data from [22,30].

We have made an average of the cross sections between 1300 to 1500 MeV c.m. energy in order to compare with the experiment. We observe that the trend of the data is well reproduced, but the absolute value is a little lower reflecting the discrepances with the data in fig. 8 in that range of energies.

In fig. 10 we show some results which can be a guideline for an experimental analysis. We concentrate on a hypothetical measurement that strengtens the contribution of the Kroll Ruderman term in order to optimize the chances to obtain an accurate value for the contact form factor $F_c(q^2)$. This can be accomplished by fixing the energy of the π^- and hence putting the Δ^{++} on shell in the diagram D.1 of fig. 1. In fig. 10 we take $m_\pi \leq \omega_{\pi^-} \leq m_\pi + 10$ MeV and show the results obtained for different Q^2 selecting the Kroll Ruderman term alone, this term plus the interference with the $N^*(1520)$ and the total

contribution. We see indeed that this magnitude is largely dominated by the Kroll Ruderman term. However the interference with the $N^*(1520)$ term is always present. Since the weight of the $N^*(1520)$ propagator is smaller at lower energies, we can also see that the region to the left of the Δ peak which appears in the figure is more suited to pin down the contribution of the Kroll Ruderman term. Yet, even at this lower energies the contribution of the interference term is still of the order of 20 per cent. This means that the accurate evaluation of $F_c(q^2)$ at level better than 20 per cent requires a careful analysis in which the interference term is explicitly considered.

6 Conclusions

We have calculated cross sections for the $\gamma_v p \to \Delta^{++}\pi^-$ and $\gamma_v p \to \Delta^0\pi^+$ reactions, extending the model of ref. [2] to virtual photons and selecting the diagrams which have a Δ in the final state.

The present calculations and comparison with the scarce experimental data are sufficient to establish the fairness of the present model to deal with the $\Delta\pi$ production process. In summary we could remark the following points:

Even if the data are scarce the agreement with them is good up to W$\simeq$ 1.6 GeV and $Q^2 \simeq 1.4\ GeV^2$ for the Δ^{++} channel. However, it would be desirable to have data for different values of Q^2. In the future such experiments are bound to be made in Thomas Jefferson Laboratory and other experimental facilities. Also other channels should be measured as well as total cross sections for $\gamma_v N \to \pi\pi N$ where the πN are not in a Δ state.

We have also shown that the peak in the cross section is due to an interference between the Δ Kroll Ruderman term and the $N^*(1520)$ excitation process followed by $\Delta\pi$ decay. This interference appeared in real photons and is not destroyed for virtual ones in spite of the fact that the electromagnetic form factors of the respective mechanisms are not exactly the same. In addition, the contribution from the longitudinal couplings in the terms involved in the interference does not destroy this effect. The experiments show clearly that interference of the two mechanisms is contructive below the $N^*(1520)$ pole, which is consistent with the findings in real photons and predictions of the relativized quark models.

Different sets of form factors have been used in our model in order to show the sensitivity of the results to these changes. These tests should be useful in view of the coming data and the possibility to extract relevant information from them.

Some plots can be useful for the experimental task. We have shown the separation of the transverse and longitudinal cross sections and found that the transverse one largely dominates the cross sections.

We have also shown a method aimed at obtaining the form factor for the Kroll Ruderman term selecting a kinematics which maximizes its importance. Even then we saw that an accurate extraction of this form factor requires the

explicit inclusion of the $N^*(1520)$ term in the analysis because of the important interference of this term with the Kroll Ruderman one.

Finally, it is also interesting to note that the present model is just part of a more general $\gamma_v N \to \pi\pi N$ model which selects only the terms where a πN pair of the final state appears forming a Δ state. Both experiments and theoretical calculations on the different $(\gamma_v, \pi\pi)$ channels should be encouraged.

Acknowledgements. We would like to thank J.A. Gómez-Tejedor, F. Cano and L. Alvarez-Ruso for useful discussions. We would like to acknowledge partial financial support for DGICYT contract number PB96-0753. One of us, J.C.N. would like to acknowledge the support from the Ministerio de Educacion y Cultura.

A1. Lagrangians.

$$L_{\pi NN} = -\frac{f}{\mu}\overline{\Psi}\gamma^{\mu}\gamma_5\partial_{\mu}\vec{\phi}\cdot\vec{\tau}\Psi \tag{28}$$

$$L_{\Delta\pi N} = -\frac{f^*}{\mu}\Psi^{\dagger}_{\Delta}S^{\dagger}_i(\partial_i\phi^{\lambda})T^{\lambda\dagger}\Psi_N + h.c. \tag{29}$$

$$L_{\Delta\Delta\pi} = -\frac{f_{\Delta}}{\mu}\Psi^{\dagger}_{\Delta}S_{\Delta i}(\partial_i\phi^{\lambda})T^{\lambda}_{\Delta}\Psi_{\Delta} + h.c. \tag{30}$$

$$L_{N^*\Delta\pi} = -\frac{g_{N^*\Delta\pi}}{\mu}\Psi^{\dagger}_{\Delta}S^{\dagger}_i(\partial_i\phi^{\lambda})T^{\lambda\dagger}\Psi_{N^*} + h.c. \tag{31}$$

$$L_{N^{*\prime}\Delta\pi} = i\overline{\Psi}_{N^{*\prime}}(\tilde{f}_{N^{*\prime}\Delta\pi} - \frac{\tilde{g}_{N^{*\prime}\Delta\pi}}{\mu^2}S^{\dagger}_i\partial_i S_j\partial_j)\phi^{\lambda}T^{\lambda\dagger}\Psi_{\Delta} + h.c. \tag{32}$$

$$L_{NN\gamma} = -e\overline{\Psi}_N(\gamma^{\mu}A_{\mu} - \frac{\chi_N}{2m}\sigma^{\mu\nu}\partial_{\nu}A_{\mu})\Psi_N \tag{33}$$

$$L_{\pi\pi\gamma} = ie(\phi_+\partial^{\mu}\phi_- - \phi_-\partial^{\mu}\phi_+)A_{\mu} \tag{34}$$

Instead of writing the explicit expressions for the terms involving the photon and the excitation of resonances like $L_{\Delta N\gamma}$, $L_{N^*N\gamma}$, $L_{\Delta\pi\gamma N}$ and $L_{N^{*\prime}N\gamma}$, we address the reader directly to eqs. (40, 43-44, 50, 51-52) respectively which provide the vertex function ($L \to -V^{\mu}\epsilon_{\mu}$).

In the former expressions $\vec{\phi}$, Ψ, Ψ_{Δ}, Ψ_{N^*}, $\Psi_{N'^*}$ and A_{μ} stand for the pion, nucleon, Δ, N^*, N'^* and photon fields, respectively ; N^* and N'^* stand for the $N^*(1440)$ and $N^*(1520)$; resonances m and μ are the nucleon and the pion masses; $\vec{\sigma}$ and $\vec{\tau}$ are the spin and isospin 1/2 operators; $\vec{S}^{\dagger}$ and $\vec{T}^{\dagger}$ are the transition spin and isospin operators from 1/2 to 3/2 with the normalization

$$\langle\frac{3}{2},M|S^{\dagger}_{\nu}|\frac{1}{2},m\rangle = C(\frac{1}{2},1,\frac{3}{2};m,\nu,M) \tag{35}$$

with ν in spherical base, and the same for $T^{\dagger}$. The operators $\vec{S}_{\Delta}$ and $\vec{T}_{\Delta}$ are the ordinary spin and isospin matrices for the a spin and isospin 3/2 object. For the pion fields we used the Bjorken and Drell convention :

$$\phi_+ = \frac{1}{\sqrt{2}}(\phi_1 - i\phi_2) \quad destroys \quad \pi^+, creates \quad \pi^- \tag{36}$$

$$\phi_- = \frac{1}{\sqrt{2}}(\phi_1 + i\phi_2) \quad destroys \quad \pi^-, creates \quad \pi^+ \tag{37}$$

$$\phi_0 = \phi_3 \quad destroys \quad \pi^0, creates \quad \pi^0 \tag{38}$$

Hence the $|\pi^+\rangle$ state corresponds to $-|11\rangle$ in isospin base.
In all formulae we have assumed that $\sigma^i \equiv \sigma_i$, $S^i \equiv S_i$, $T^i \equiv T_i$ are Euclidean vectors. However for ∂_i, A_i, p_i, etc, we have respected their covariant meaning.

A2. Feynman Rules.

Here we write the Feynman rules for the different vertices including already the electromagnetic form factors. We assumed the photon with momenta q as an incoming particle while the pion with momentum k is an outgoing particle in all vertices. The momentum p, p' are those of the baryonic states just before and after the photon absorption vertex (or pion production vertex in eq. (42)).

$$V^{\mu}_{\gamma NN} = -ie \left\{ \begin{array}{c} F_1^N(q^2) \\ F_1^N(q^2)[\frac{\vec{p}+\vec{p}'}{2m}] + i\frac{\vec{\sigma}\times\vec{q}}{2m} G_M^N(q^2) \end{array} \right\} \tag{39}$$

$$V^{\mu}_{\gamma N\Delta} = \sqrt{\frac{2}{3}} \frac{f_\gamma(q^2)}{m_\pi} \frac{\sqrt{s}}{m_\Delta} \left\{ \begin{array}{c} \frac{\vec{p}_\Delta}{\sqrt{s}}(\vec{S^\dagger} \times \vec{q}) \\ \frac{p^0_\Delta}{\sqrt{s}}[\vec{S^\dagger} \times (\vec{q} - \frac{q^0}{p^0_\Delta}\vec{p_\Delta})] \end{array} \right\} \tag{40}$$

$$V_{\pi N\Delta} = -\frac{f^*}{\mu} \vec{S^\dagger} \cdot (\vec{k} - \frac{k^0}{\sqrt{s}}\vec{p_\Delta}) T^{\lambda\dagger} \tag{41}$$

$$V_{\pi NN} = -\frac{f}{\mu}(\vec{\sigma}\vec{k} - k^0 \frac{\vec{\sigma}(\vec{p}+\vec{p}')}{2m})\tau^\lambda \tag{42}$$

$$V^0_{N^*N\gamma} = i\frac{\vec{q}^{\,2}}{2m} F_2(q^2) - i\vec{q}^{\,2}(1 + \frac{q^0}{2m}) F_1(q^2) \tag{43}$$

$$\begin{aligned} V^i_{N^*N\gamma} = {} & F_2(q^2)[i\vec{q}\,\frac{q^0}{2m} + (\vec{\sigma}\times\vec{q})(1+\frac{q^0}{2m})] \\ & -F_1(q^2)[i\vec{q}q^0(1+\frac{q^0}{2m}) + q^2\frac{1}{2m}(\vec{\sigma}\times\vec{q})] \end{aligned} \tag{44}$$

$$V_{N^*\Delta\pi} = -\frac{g_{N^*\Delta\pi}}{\mu} \vec{S^\dagger} \cdot \vec{k} T^{\lambda\dagger} \tag{45}$$

$$V_{\Delta\Delta\pi} = -\frac{f_\Delta}{\mu} \vec{S_\Delta} \cdot \vec{k}\, T^\lambda_\Delta \tag{46}$$

$$V_{N^{*\prime}\Delta\pi} = -(\tilde{f}_{N^{*\prime}\Delta\pi} + \frac{\tilde{g}_{N^{*\prime}\Delta\pi}}{\mu^2} \vec{S^\dagger} \cdot \vec{k} \vec{S} \cdot \vec{k}) T^{\lambda\dagger} \tag{47}$$

$$V^{\mu}_{\gamma\Delta\Delta} = -i \left\{ \begin{array}{c} e_\Delta F_1^\Delta(q^2) \\ e_\Delta F_1^\Delta(q^2)[\frac{\vec{p}+\vec{p}'}{2m_\Delta}] + i\frac{\vec{S_\Delta}\times\vec{q}}{3m} e G_M^\Delta(q^2) \end{array} \right\} \tag{48}$$

$$V^{\mu}_{\pi\pi\gamma} = -iq_\pi(k^\mu + k'^\mu) F_{\gamma\pi\pi}(q^2) \tag{49}$$

$$V^{\mu}_{\Delta N\gamma\pi} = -q_{\pi}\frac{f^*}{m_{\pi}}T^{\lambda\dagger}\left\{\begin{array}{c}\vec{S}^{\dagger}\,\frac{\vec{p}_{\Delta}}{\sqrt{s}}\\ \vec{S}^{\dagger}\end{array}\right\}F_c(q^2) \tag{50}$$

$$V^{0}_{\gamma NN'^*} = i(G_1(q^2) + G_2(q^2)p'^0 + G_3(q^2)q^0)\vec{S}^{\dagger}\cdot\vec{q} \tag{51}$$

$$\begin{aligned} V^{i}_{\gamma NN'^*} = -i[(\frac{G_1(q^2)}{2m} - G_3(q^2))(\vec{S}^{\dagger}\cdot\vec{q})\,\vec{q} - iG_1(q^2)\frac{\vec{S}^{\dagger}\cdot\vec{q}}{2m}(\vec{\sigma}\times\vec{q}) \\ -\vec{S}^{\dagger}\{G_1(q^2)(q^0 + \frac{\vec{q}^{\,2}}{2m}) + G_2(q^2)p'^0q^0 + G_3(q^2)q^2\}] \end{aligned} \tag{52}$$

A3. Coupling and form factors

Coupling constants :

$f = 1 \qquad f^* = 2.13$

$f_{\Delta N\gamma} = 0.122 \qquad f_\Delta = 0.802$

$e = 0.3027$

$\tilde{f}_{N^{*\prime}\Delta\pi} = -0.911 \qquad \tilde{g}_{N^{*\prime}\Delta\pi} = 0.552$

$g_{N^*\Delta\pi} = 2.07$

Form factors :

For the off-shell pions we use a form factor of the monopole type :

$$F_\pi(p^2) = \frac{\Lambda_\pi^2 - \mu^2}{\Lambda_\pi^2 - p^2} \qquad ; \Lambda_\pi \sim 1250\, MeV \tag{53}$$

The Sachs's form factors are given by

$$G_M^N(q^2) = \frac{\mu_N}{(1 - \frac{q^2}{\Lambda^2})^2} \qquad ; G_E^N(q^2) = \frac{1}{(1 - \frac{q^2}{\Lambda^2})^2} \tag{54}$$

with $\Lambda^2 = 0.71\ GeV^2$; $\mu_p = 2.793$; $\mu_n = -1.913$.

The relation between $F_1^p(q^2)$ (Dirac's form factor) and $G_E^p(q^2)$ is :

$$F_1^p(q^2) = G_E^p(q^2)\frac{(1 - \frac{q^2\mu_p}{4m_N^2})}{(1 - \frac{q^2}{4m_N^2})} \tag{55}$$

and $F_1^n = 0$.

For the delta resonance we use

$$F_1^\Delta = F_1^p(q^2) \tag{56}$$

$$G_M^\Delta(q^2) = \frac{\mu_\Delta}{(1 - \frac{q^2}{\Lambda^2})^2} \tag{57}$$

In the case of the Δ^{++} we make use of the experimental value $\mu_{\Delta^{++}} = 1.62$ μ_p and for the other charge states we make use of the ratio ($e > 0$):

$$\frac{\mu_\Delta}{\mu_p} = \frac{e_\Delta}{e} \tag{58}$$

For the $\gamma\pi\pi$ vertex in diagram D2, we take the form factor:

$$F_{\gamma\pi\pi}(q^2) = \frac{1}{(1 - \frac{q^2}{\lambda_\pi^2})} \tag{59}$$

with $\lambda_\pi^2 = 0.5\ GeV^2$.

The axial nucleon form factor is given by:

$$F_A(q^2) = \frac{1}{(1 - \frac{q^2}{M_A^2})^2} \tag{60}$$

with $M_A = 1.16$ GeV. This form factor is used for the contact form factor, $F_c(q^2)$, in some of the results reported here. Some others results use $F_c(q^2) = F_{\gamma\pi\pi}(q^2)$.

The form factor for the $\gamma\Delta N$ transition is taken as:

$$f_\gamma(q^2) = f_\gamma(0) \frac{(1 - \frac{q^2}{(m_\Delta + m)^2})}{(1 - \frac{q^2 \mu_p}{4m_N^2})} \frac{G_M^p(q^2)}{\mu_p} \frac{(m_\Delta + m)^2}{(m_\Delta + m)^2 - q^2} \tag{61}$$

where $f_\gamma(0) = 0.122$

A4. Amplitudes for the reaction

In this appendix we write the explicit expressions for the amplitudes of the Feynman diagrams used in the model. The isospin coefficients and some constant factors are collected in the coefficients C which are written in the table A4.

Reaction	D1	D2	D3	D4	D5	D6	D7	D8
$\gamma_v p \to \pi^- \Delta^{++}$	-i/3	-i/3	0	i/3	1	i/3	i	-1
$\gamma_v p \to \pi^+ \Delta^0$	i/9	i/9	-2i/9	i/9	-2/3	0	i/3	-1/3

Table A4: Coefficients of the amplitudes for the Δ^{++} and Δ^0 ($\Delta^0 \to \pi^- p$) reactions, accounting for isospin and constant factors.

In the following expressions q, p_1, p_2, p_4, and p_5 are the momentum of the photon,the incoming nucleon, the outgoing nucleon and the two pions :

γ	p	π^+	π^-	p
q	p_1	p_5	p_4	p_2

We write only the amplitude when the pion labelled p_5 is emitted before the pion labelled p_4(Δ^0 case), except in the case of the D6 where the only

possibility is the Δ^{++} and the explicit amplitude for this case is written. We have also evaluated the crossed diagrams when the pion labelled p_5 is emitted after the pion called p_4(Δ^{++} case). Such amplitudes are exactly the same than the others written before, but exchanging the momenta p_4 and p_5 and changing some isospin coefficient. This latter change is taken into account by the factor C written in table A4.

We should note that in the vertex $\Delta N\pi$, when $\vec{p}_\Delta$ is not zero, we must change $\vec{p}_\pi$ by $\vec{p}_\pi - \frac{p^0}{\sqrt{s}}\vec{p}_\Delta$ for the final pion.

In the formulae, D_π, G_Δ, G_N, G_{N^*}, $G_{N'^*}$ are the propagator of the pion, delta, nucleon, $N^*(1440)$, $N^*(1520)$ respectively. Expressions for them and for the width of the resonances can be found in [1, 2, 14].

$$
\begin{aligned}
-iT_1^\mu &= Ce(\frac{f^*}{\mu})^2 G_\Delta(p_2+p_4)F_\pi((p_5-q)^2)F_c(q^2) \qquad (62)\\
&\times \left\{ \begin{array}{c} [2\vec{p}_4\cdot\vec{p}_5 - i(\vec{p}_4\times\vec{p}_5)\cdot\vec{\sigma}]\frac{-1}{\sqrt{s_\Delta}} \\ 2\vec{p}_4 - i(\vec{\sigma}\times\vec{p}_4) \end{array} \right\}\\
-iT_2^\mu &= Ce(\frac{f^*}{\mu})^2 G_\Delta(p_2+p_4)D_\pi(p_5-q)F_\pi((p_5-q)^2)F_{\gamma\pi\pi}(q^2) \qquad (63)\\
&\times[2\vec{p}_4\cdot(\vec{p}_5-\vec{q}) - i(\vec{p}_4\times(\vec{p}_5-\vec{q}))\cdot\vec{\sigma}]\\
&\times \left\{ \begin{array}{c} 2p_5 - q \end{array} \right\}^\mu\\
-iT_3^\mu &= C\frac{f}{\mu}\frac{f^*}{\mu}\frac{f_\gamma(q^2)}{\mu}G_N(p_2+p_4)G_\Delta(p_1+q) \qquad (64)\\
&\times \left\{ \begin{array}{c} [-2i(\vec{p}_4\times\vec{q}) - (\vec{\sigma}\cdot\vec{q})\vec{p}_4 + (\vec{p}_4\cdot\vec{q})\vec{\sigma}]\frac{\vec{p}_\Delta}{m_\Delta} \\ [-2i(\vec{p}_4\times\vec{q}') - (\vec{\sigma}\cdot\vec{q}')\vec{p}_4 + (\vec{p}_4\cdot\vec{q}')\vec{\sigma}]\frac{p^0_\Delta}{m_\Delta} \end{array} \right\}\\
&\times[-p_5^0\frac{\vec{\sigma}(2\vec{p}_1-\vec{p}_5)}{2m} + \vec{\sigma}\vec{p_5}]
\end{aligned}
$$

with $\vec{q}' = (\vec{q} - \frac{q^0}{p^0_\Delta}\vec{p_\Delta})$

$$
\begin{aligned}
-iT_4^\mu &= Ce(\frac{f^*}{\mu})^2 G_N(p_1+k)G_\Delta(p_2+p_4)F_\pi((p_5-q)^2) \qquad (65)\\
&\times[2\vec{p}_4\cdot\vec{p}_5 - i(\vec{p}_4\times\vec{p}_5)\cdot\vec{\sigma}]\\
&\times \left\{ \begin{array}{c} F_1^p(q^2) \\ F_1^p(q^2)[\frac{\vec{p}+\vec{p}'}{2m}] + iG_M^p(q^2)\frac{\vec{\sigma}\times\vec{q}}{2m} \end{array} \right\}
\end{aligned}
$$

$$-iT_5^0 = 0 \quad in \quad \gamma - p \quad CM \quad frame \qquad (66)$$

$$
\begin{aligned}
-iT_5^i &= C\frac{f^*}{\mu}\frac{f_\Delta}{\mu}\frac{f_\gamma(q^2)}{\mu}G_\Delta(p_2+p_4)G_\Delta(p_1+q) \qquad (67)\\
&\times[i\frac{5}{6}(\vec{p}_4\cdot\vec{q})\vec{p}_5 - i\frac{5}{6}(\vec{p}_5\cdot\vec{q})\vec{p}_4 - \frac{1}{6}(\vec{p}_4\cdot\vec{p}_5)(\vec{\sigma}\times\vec{q}) -\\
&\frac{1}{6}(\vec{p}_4\cdot\vec{\sigma})(\vec{p}_5\times\vec{q}) + \frac{2}{3}(\vec{p}_5\cdot\vec{\sigma})(\vec{p}_4\times\vec{q})]
\end{aligned}
$$

$$-iT_6^0 = C(\frac{f^*}{\mu})^2 G_\Delta(p_2+p_5)G_\Delta(p_1-p_4)F_\pi((p_5-q)^2)\{e_\Delta F_1^\Delta(q^2) \times[2\vec{p}_5\cdot\vec{p}_4 - i(\vec{p}_5\times\vec{p}_4)\cdot\vec{\sigma}]\} \quad (68)$$

$$\begin{aligned} -iT_6^i &= C(\frac{f^*}{\mu})^2 G_\Delta(p_2+p_5)G_\Delta(p_1-p_4)F_\pi((p_5-q)^2) \\ &\times\{\frac{e_\Delta F_1^\Delta(q^2)}{2}\frac{(\vec{p}_1-2\vec{p}_4)}{m_\Delta}[2\vec{p}_5\cdot\vec{p}_4 - i(\vec{p}_5\times\vec{p}_4)\cdot\vec{\sigma}] + \\ &i\frac{eG_M^\Delta(q^2)}{m}[i\frac{5}{6}(\vec{p}_4\cdot\vec{q})\vec{p}_5 - i\frac{5}{6}(\vec{p}_5\cdot\vec{q})\vec{p}_4 - \frac{1}{6}(\vec{p}_5\times\vec{q})(\vec{p}_4\cdot\vec{\sigma}) - \\ &\frac{1}{6}(\vec{p}_5\cdot\vec{\sigma})(\vec{p}_4\times\vec{q}) + \frac{2}{3}(\vec{p}_5\cdot\vec{p}_4)(\vec{\sigma}\times\vec{q})]\} \end{aligned} \quad (69)$$

Amplitude of N'^*(1520):
Vector part :

$$\begin{aligned} -iT_7^i &= C\frac{f^*}{\mu}G_\Delta(p_2+p_4)G_{N'^*}(p_1+q) \\ &\times\vec{S}\cdot\vec{p}_4[\tilde{f}_{N'^*\Delta\pi} + \frac{\tilde{g}_{N'^*\Delta\pi}}{\mu^2}\vec{S}^\dagger\cdot\vec{p}_5\vec{S}\cdot\vec{p}_5] \\ &\times\{(\frac{G_1(q^2)}{2m} - G_3(q^2))(\vec{S}^\dagger\cdot\vec{q})\,\vec{q} - iG_1(q^2)\frac{\vec{S}^\dagger\cdot\vec{q}}{2m}(\vec{\sigma}\times\vec{q}) \\ &-\vec{S}^\dagger[G_1(q^2)(q^0+\frac{\vec{q}^{\,2}}{2m}) + G_2(q^2)p'^0q^0 + G_3(q^2)q^2]\} \end{aligned} \quad (70)$$

scalar part:

$$\begin{aligned} -iT_7^0 &= -C\frac{f^*}{\mu}G_\Delta(p_2+p_4)G_{N'^*}(p_1+q) \\ &\times\vec{S}\cdot\vec{p}_4[\tilde{f}_{N'^*\Delta\pi} + \frac{\tilde{g}_{N'^*\Delta\pi}}{\mu^2}\vec{S}^\dagger\cdot\vec{p}_5\vec{S}\cdot\vec{p}_5] \\ &\times[G_1(q^2) + G_2(q^2)p'^0 + G_3(q^2)q^0]\vec{S}^\dagger\cdot\vec{q} \end{aligned} \quad (71)$$

Amplitude of N^*(1440):
Vector part :

$$\begin{aligned} -iT_8^i &= C\frac{f^*}{\mu}\frac{g_{N^*\Delta\pi}}{\mu}G_\Delta(p_2+p_4)G_{N^*}(p_1+q)\vec{S}\cdot\vec{p}_4\vec{S}^\dagger\cdot\vec{p}_5 \\ &\times\ \{F_2(q^2)[i\vec{q}\,\frac{q^0}{2m} + (\vec{\sigma}\times\vec{q})(1+\frac{q^0}{2m})] \\ &-F_1(q^2)[i\vec{q}q^0(1+\frac{q^0}{2m}) + q^2\frac{1}{2m}(\vec{\sigma}\times\vec{q})]\} \end{aligned} \quad (72)$$

scalar part:

$$-iT_8^0 = C\frac{f^*}{\mu}\frac{g_{N^*\Delta\pi}}{\mu}\, G_\Delta(p_2+p_4)G_{N^*}(p_1+q)\vec{S}\cdot\vec{p}_4\vec{S}^\dagger\cdot\vec{p}_5 \times \{i\frac{\vec{q}^{\,2}}{2m}F_2(q^2) - i\vec{q}^{\,2}(1+\frac{q^0}{2m})F_1(q^2)\} \quad (73)$$

A5. Amplitudes for the gauge invariant set within Berends formalism.

The explicit amplitudes for the gauge invariant set of the 4 diagrams D1, D2, D4 and D6, in the presence of different form factors are made according to eq. (17) of [25]. We implement them in our formalism by making the following substitutions in the amplitudes shown in the appendix A4. The form factor in the zeroth component of each amplitude is changed as:

T_1^μ:

$$\frac{\vec{S}^\dagger\cdot\vec{p}_\Delta}{\sqrt{s_\Delta}}F_c \to \frac{\vec{S}^\dagger\cdot\vec{p}_\Delta}{\sqrt{s_\Delta}}F_c - (F_c-1)(\frac{\vec{S}^\dagger\cdot\vec{p}_\Delta}{\sqrt{s_\Delta}}q^0 - \vec{S}^\dagger\cdot\vec{q})\frac{q^0}{q^2} \quad (74)$$

T_2^μ :

$$F_{\gamma\pi\pi}\{2p_5-q\}^0 \to F_{\gamma\pi\pi}\{2p_5-q\}^0 + (F_{\gamma\pi\pi}-1)D_\pi^{-1}\frac{q^0}{q^2} \quad (75)$$

T_4^μ :

$$F_1^p \to F_1^p + (F_1^p-1)G_N^{-1}\frac{q^0}{q^2} \quad (76)$$

T_6^μ :

$$F_1^{\Delta^{++}} \to F_1^{\Delta^{++}} + (F_1^{\Delta^{++}}-1)G_\Delta^{-1}\frac{q^0}{q^2} \quad (77)$$

where G_N, G_Δ are the non relativistic propagator of the nucleon and the Δ resonance and D_π the ordinary relativistic pion propagator.

A6. Miscellaneous Formulae.

In order to obtain our amplitudes we have employed some useful relations:

$$\sum_M S_i|M\rangle\langle M|S_j^\dagger = \frac{2}{3}\delta_{ij} - \frac{i}{3}\epsilon_{ijk}\sigma_k = \delta_{ij} - \frac{1}{3}\sigma_i\sigma_j \quad (78)$$

$$\sum_{MM'} S_i|M\rangle\langle M|S_{\Delta j}|M'\rangle\langle|M'|S_k^\dagger = \frac{5}{6}i\epsilon_{ijk} - \frac{1}{6}\delta_{ij}\sigma_k + \frac{2}{3}\delta_{ik}\sigma_j - \frac{1}{6}\delta_{jk}\sigma_i \tag{79}$$

From eqs. (78) and (79). we can prove the following relations,which are used in the calculation of the amplitudes:

$$\vec{S}\cdot\vec{p}\vec{S^\dagger}\cdot\vec{q} = \frac{1}{3}[2\vec{p}\cdot\vec{q} - i(\vec{p}\times\vec{q})\cdot\vec{\sigma}] \tag{80}$$

$$\begin{aligned}\vec{S}\cdot\vec{p}(\vec{S_\Delta}\times\vec{k})\cdot\vec{\epsilon}\vec{S^\dagger}\cdot\vec{q} = [&\frac{5}{6}i\vec{p}\cdot\vec{\epsilon}\vec{q}\cdot\vec{k} - \frac{5}{6}i\vec{p}\cdot\vec{k}\vec{q}\cdot\vec{\epsilon} - \\ &\frac{1}{6}(\vec{p}\times\vec{k})\cdot\vec{\epsilon}\vec{\sigma}\cdot\vec{q} - \frac{1}{6}\vec{\sigma}\cdot\vec{p}(\vec{q}\times\vec{k})\cdot\vec{\epsilon} + \\ &\frac{2}{3}\vec{p}\cdot\vec{q}(\vec{\sigma}\times\vec{k})\cdot\vec{\epsilon}]\end{aligned} \tag{81}$$

where we have omitted the sum over intermediate states.

References

[1] J.A. Gómez-Tejedor and E. Oset, Nucl. Phys. A571 (1994) 667.

[2] J.A. Gómez-Tejedor and E. Oset, Nucl. Phys. A600 (1996) 413.

[3] A. Braghieri et al., Phys. Lett. B363 (1995) 46.

[4] A. Zabrodin et al., Phys. Rev. C55 (1997) 1617.

[5] F. Härter et al., Phys. Lett. B401 (1997) 229.

[6] L.Y. Murphy and J.M. Laget, DAPHNIA/sphN 95-42, preprint.

[7] J.M. Laget, private communication

[8] K. Ochi, M. Hirata and T. Takaki, Phys. Rev. C56 (1997) 1472.

[9] M. Hirata, K. Ochi and T. Takaki, nucl-th/9711017.

[10] M. Benmerrouche and E. Tomusiak, Phys. Rev. Lett. 73 (1994) 400.

[11] V. Bernard, N. Kaiser, Ulf-G. Meissner and A. Schmidt, Nucl. Phys. A 580. (1994) 475.

[12] V. Bernard, N. Kaiser, and Ulf-G. Meissner, Phys. Rev. Lett.74 (1995) 1036.

[13] M. Benmerrouche and E. Tomusiak, Phys. Rev. Lett. 74 (1995) 1037.

[14] J.A. Gómez-Tejedor, F. Cano and E. Oset, Phys. Lett. B379 (1996) 39.

[15] R. Koniuk and N. Isgur, Phys. Rev. D21 (1980) 1868.

[16] S. Capstick and W. Roberts, Phys. Rev. D49 (1994) 4570.

[17] F. Cano, P. González, B. Desplanques and S. Noguera, Z. Phys. A359 (1997) 819.

[18] J.A. Gómez-Tejedor, M.J. Vicente-Vacas and E. Oset, Nucl. Phys. A588 (1995)

[19] B. Krusche, private communication

[20] S. Kamalov and E. Oset ,Nucl. Phys. A625 (1997) 873.

[21] J.A. Gómez Tejedor, S. Kamalov and E. Oset, Phys. Rev. C54 (1996) 3160.

[22] K. Wacker and G. Drews, Nucl. Phys. B144 (1978) 274,282.

[23] V.Burkert, private communication.

[24] A. Bartl, K. Wittmann, N. Paver, and C. Verzegnassi, Il Nuovo Cimento, 45A(1978) 457

[25] F.A. Berends and R. Gastmans, Phys. Rev. D5 (1972) 204

[26] R.C.E. Devenish, T.S. Eisenschitz and J. G. Korner, Phys. Rev. D11 (1976) 3063.

[27] M. Warns, H. Schröder, W. Pfeil and H. Rollnik, Z. Phys. 45 (1990) 627.

[28] P.J. Mulders, Phys. Reports 185 (1990) 83.

[29] A. Gil and E. Oset, Nucl. Phys. A850 (1994) 513.

[30] E. Amaldi,S. Fubini and G. Furlan, Pion electroproduction, Springer Tracts in Modern Physics, Vol. 83 (Springer, Berlin, 1979)

[31] S. Nozawa and T.S.H. Lee, Nucl. Phys. A513 (1990) 511.

[32] L. Alvarez, S.K. Singh, M.J. Vicente-Vacas, Phys. Rev. C57 (1998) 2693

[33] C. E. Carlson, N. Mukhopadhyay, Phys. Rev. Lett. 13(1998) 2646

[34] C. E. Carlson, Phys. Rev. D34 (1986) 2704

[35] P. Stoler, Phys. Rep. 226 (1993)103

[36] Z. Li, V. Burkert and Z. Li, Phys. Rev. D46 (1992) 70

[37] C. Gerhardt, Z. Phys. C4(1980) 311

[38] V. Burkert, private communication.

[39] A. Gil, J. Nieves, E. Oset, Nucl. Phys. A627 (1997) 553.

[40] H-D. Kiehlmann et al, J. Phys. G:Nucl. Phys. 7(1981) 709-724 and 725-735.

[41] C. Driver et al, Nucl. Phys. B32(1971)45-65.

[42] H.E. Montgomery et al, Nucl. Phys. B51(1973)377-387

[43] A. Bartl et al, Nuovo Cimento 12 (1972) 703

[44] P. Joos et al, Phys. Lett. B62 (1976) 230

[45] Adler et al, Phys. Rev. 169(1967) 1392

[46] P. Carruthers et al, Phys. Lett. B24 (1967) 464

[47] A. Bartl et al, Z. Physik, 269 (1974) 399-406

[48] Aachen-Berlin-Bonn-Hamburg-Heidelberg collaboration, Phys. Rev. 175 (1968) 1669.